The monoallelic deletion of protein arginine methyltransferase 1 in activated B cells elevates the antibody response and confers a B cell-intrinsic fitness advantage

Michael Slattery

Supervisor: Dr. Javier M Di Noia

Date of Submission: January 2025

Faculty of Medicine

Department of Microbiology & Immunology

McGill University, Montreal QC

A thesis submitted to McGill University in partial fulfillment of the requirements of the degree of Master of Science (MSc)

Table of Contents

Abstract 3
Résumé 4
Acknowledgements 5
Contributions of Authors 5
Abbreviations 6
Chapter I: Introduction 7
1.1 B Lymphocytes 7
1.2 Antibody Structure and Isotypes 7
1.3 The Germinal Centre Response 9
1.4 Germinal Centre Dynamics 11
1.5 Protein Arginine Methylation 15
1.6 Research Question and Aims 19
Chapter II: Materials and Methods 22
Chapter III: Results 29
3.1 The partial loss of *Prmt1* in activated B cells elevates proportions of splenic GCB cells.. 29
3.2 Antibody production and plasma cell differentiation are elevated in *Prmt1*$^{+/-}$ Cγ1-cre mice 31
3.3 *Prmt1* protein dosage restricts the fitness and differentiation of GCB cells and PCs 35
3.4 IL-4 and IL-21 differentially control the fitness of *Prmt1*$^{+/-}$ Cγ1-cre and *Prmt1*$^{-/-}$ Cγ1-cre iGBs 39
Chapter IV: Discussion 52
Conclusion 60
Supplementary Tables 61
Table S1: Antibodies used for flow cytometry and ELISAs. 61
Table S2: Antibodies used for Western blotting. 62
References 63

List of Figures & Tables

Figure 1: The monoallelic deletion of *Prmt1* in activated B cells increases frequencies of GCB cells in the spleen 30

Figure 2: Antibody production and plasma cell frequencies are elevated in *Prmt1*$^{+/-}$ Cγ1-cre mice 33

Figure 3: *Prmt1*$^{+/-}$ Cγ1-cre B cells have an intrinsic fitness advantage 36

Figure 4: IL-21 augments the fitness of *Prmt1*$^{+/-}$ Cγ1-cre and *Prmt1*$^{-/-}$ Cγ1-cre B cells..... 41

Supplementary Figure 1: Flow cytometry gating strategies for assessing frequencies of splenic GCB cells, T_{FH} and T_{FR} cells, and PCs..... 43

Supplementary Figure 2: Splenic B cell and T cell populations in immunized *Prmt1*$^{+/-}$ Cγ1-cre mice..... 44

Supplementary Figure 3: Memory responses are intact in *Prmt1*$^{+/-}$ Cγ1-cre mice..... 45

Supplementary Figure 4: *Prmt1* is haplo-sufficient for supporting normal B cell proliferation and differentiation..... 47

Supplementary Figure 5: *Prmt1*$^{+/-}$ Cγ1-cre iGBs are poised for PC differentiation..... 49

Supplementary Figure 6: *Prmt1*-deficient B cells are prone to BCR-induced growth inhibition and PC differentiation..... 50

Supplementary Table 1: Antibodies used for flow cytometry and ELISAs..... 61

Supplementary Table 2: Antibodies used for Western blotting..... 62

Abstract

Within germinal centres (GC), B cells undergo a Darwinian process of mutation and selection to generate high-affinity antibodies, eventually differentiating into plasma cells (PCs) to secrete those antibodies. Protein arginine methyltransferase 1 (PRMT1) is a critical regulator of GC responses. PRMT1 promotes GCB cell expansion by opposing PC differentiation. PRMT1 also promotes the growth of GCB cell-like lymphoma cell lines. However, inhibiting its activity in patients with GC-derived lymphomas has proven ineffective, warranting further investigations of PRMT1 in GCB cells. Here, we find PRMT1 protein dosage dynamically controls B cell fitness. Whereas the biallelic deletion of *Prmt1* in activated mouse B cells impairs GC expansion and antibody responses, its monoallelic deletion increases the frequency of splenic GCB cells and elevates antibody production. Importantly, the heterozygous deletion of *Prmt1* confers a fitness advantage to activated B cells *ex vivo*, which is heightened by IL-21 and is associated with mTOR activation. Our work provides potential explanations for the poor efficacy of PRMT1 inhibitors against human GCB cell lymphoma.

Résumé

La génération d'anticorps est une caractéristique de l'immunité acquise qui trouve son origine dans les centres germinatifs des ganglions lymphatiques. Dans les centres germinatifs, les lymphocytes B commencent un processus darwinien de mutation, sélection et expansion qui leur permettra de secréter des anticorps de haute affinité quand ils seront finalement différenciés en plasmocytes. Protein arginine methyltransferase 1 (PRMT1) est un régulateur critique de la formation et de l'expansion des centres germinatifs. PRMT1 promeut la prolifération des lymphocytes B dans les centres germinatifs, les empêchant de se différencier prématurément en plasmocytes. PRMT1 est surexprimée dans les tumeurs malignes dérivées des centres germinatifs, mais l'inhibition de son activité chez les patients atteints de lymphomes dérivés des centres germinatifs s'est avérée infructueuse, ce qui justifie de nouvelles recherches sur PRMT1 dans les lymphocytes B. Dans le présent travail, nous constatons que le dosage de la protéine PRMT1 régule dynamiquement l'aptitude des lymphocytes B. Alors que la délétion totale de *Prmt1* dans les lymphocytes B activées de souris empêche l'expansion des centres germinatifs, sa délétion hétérozygote augmente la cellularité de lymphocytes B dans les centres germinatifs, la production d'anticorps, et de la production de plasmocytes. De plus, la délétion monoallélique de *Prmt1* est suffisante pour conférer un avantage de croissance aux lymphocytes B activés, qui est augmenté par l'interleukine-21. Nos travaux mettent en évidence la régulation des lymphocytes B par PRMT1 et fournissent des implications pour son ciblage dans les lymphomes à lymphocytes B.

Acknowledgements

First, I thank my supervisor, Dr. Javier Di Noia, for his mentorship during my graduate studies. I also thank Dr. Astrid Zahn and Dr. Silvana Ferreira for mentoring me on techniques and for supporting my project, as well as past and present lab members for making my experience in the lab enjoyable!

I would also like to thank my parents, Judy and Terry, my sister Nicole, as well as my supportive friends back at home, Hannah and Mary, for always listening to me when I needed to vent and for always being so supportive. And to my friends in Montréal — Lou, Jude, Tenzin, Alex, Jon, and Mathilde — thank you for getting me through the tougher parts of my studies. I love you all!

Contributions of Authors

This thesis was written by Michael Slattery (M.S., McGill University) and was edited by Dr. Javier Marcelo Di Noia (J.M.D., Institut de recherches cliniques de Montréal). All experiments and data analysis were executed by M.S., with the following exceptions. Dr. Astrid Zahn (A.Z., Institut de recherches cliniques de Montréal) obtained preliminary results and prepared the antigen for immunizing one cohort of mice depicted in figure 2, and Dr. Silvana Ferreira (S.F., Institut de recherches cliniques de Montréal) assisted by performing the splenocyte extractions used for experiments by M.S. in figures 3, 4 and S3 as well as by performing the Western blots of asymmetrically dimethylated arginine substrates in figures 3 and S3. S.F. also performed iGB purifications, which were used for IL-21 stimulation experiments by M.S. in figure 4.

Abbreviations

ABC: activated B cell

aDMA: asymmetric di-methylarginine

AID: activation-induced cytidine deaminase

BAFF: B-cell activating factor

BCR: B cell receptor

CD40L: CD40 ligand

sDMA: symmetric di-methylarginine

D: diversity

DLBCL: diffuse large B cell lymphoma

DZ: dark zone

Fab: fragment antigen-binding

Fc: fragment crystallizable

FDC: follicular dendritic cell

HEL: hen egg lysozyme

HL: Hodgkin lymphoma

IC: immune complex

iGB: induced germinal center B cell

Ig: immunoglobulin

IgH: immunoglobulin heavy chain

IgL: immunoglobulin light chain

IL-4: interleukin-4

IL-21: interleukin-21

GC: germinal centre

J: joining

LZ: light zone

MBC: memory B cell

MHCII: major histocompatibility complex II

MMA: mono-methylarginine

PC: plasma cell

PRMT: protein arginine methyltransferase

SHM: somatic hypermutation

T_H: T helper cell

T_{FH}: T follicular helper cell

T_{FR}: T follicular regulatory cell

V: variable

Chapter I: Introduction

1.1 B Lymphocytes

The elimination of pathogenic microorganisms from the extracellular spaces of the body depends on the humoral immune response (de simoneLu et al., 2018). The humoral immune response is orchestrated by B lymphocytes or B cells that secrete antibodies against invading pathogens. Antibodies contribute to protective immunity through the neutralization of pathogens as well as through the activation of complement (Nothelfer et al., 2015). Antibodies prevent the replication of extracellular pathogens, notably bacteria, within the extracellular spaces of the host organism (Lu et al., 2018). They also prevent intracellular pathogens from entering host cells, thus impeding their replication (Casadevall, 1998). Indeed, humans with deficiencies in antibody production are susceptible to recurrent respiratory and gastrointestinal infections (Aghamohammadi et al., 2009; Oksenhendler et al., 2008; Quinti et al., 2007).

1.2 Antibody Structure and Isotypes

Every B cell expresses a unique antibody that recognizes a specific antigen. In humans, it is estimated that the naïve antibody repertoire consists of at least 10^{15} unique potential antibody specificities (Rees, 2020). The diversity of antibodies in vertebrate organisms permits the immune system to elicit responses against a remarkable range of different antigens.

Antibodies are heterodimeric proteins, noted by their Y-shaped structure. They are composed of a pair of two identical heavy chains (IgH) and two identical light chains (IgL) connected by disulfide bridges (Edelman et al., 1969). The N-terminal region of the IgH chains dimerizes with the IgL chains to form two fragment antigen-binding (Fab) sites. The Fab sites contain a variable region domain from each IgH and IgL chain and are responsible for antigen-

binding (Fleischman et al., 1963; Inbar et al., 1972; Porter, 1959). Antibody-encoding genes are assembled during B cell development in the bone marrow through a somatic rearrangement of germline variable (V), diversity (D), and joining (J) gene segments (Bassing et al., 2002; Jung and Alt, 2004). V, D and J gene segments are recombined to assemble the antigen-binding variable region exon of the IgH chain, while the V and J gene segments are recombined to generate the antigen-binding variable region exon of the IgL chain. This process, known as V(D)J recombination, generates the vast repertoire of antibodies in vertebrate organisms and underpins the efficiency of antibody responses.

Additional antibody diversity is achieved through the constant regions of the IgH and IgL chains. The antigen-binding Fab sites are connected by a hinge region to the fragment crystallizable (Fc) region or IgH constant region, which constitutes the C-terminal portion of the dimerized IgH chains (Amzel and Poljak, 1979). There are five classes or isotypes of the IgH chain, encoded by their constant region domains: IgM, IgD, IgG, IgA, and IgE (Chaudhuri and Alt, 2004). The IgG and IgA isotypes are further divided into sub-classes depending on the vertebrate species. Humans have four IgG isotypes (IgG1, IgG2, IgG3, and IgG4) and two IgA isotypes (IgA1 and IgA2), whereas mice have four IgG isotypes (IgG1, IgG2b, IgG2c/IgG2a, and IgG3) but only one IgA isotype (Mestas and Hughes, 2004). Each IgH chain associates with either one of the two IgL chains: Igκ or Igλ (Amzel and Poljak, 1979).

Antibodies are expressed on the surface of B cells as part of larger signalling complex, called the B cell receptor (BCR). The BCR consists of the membrane-bound antibody in addition to two transmembrane signalling moieties: Igα and Igβ (Hombach et al., 1990). Mature B cells derived from the bone marrow express IgM and IgD on their surface (Geisberger et al., 2006). In the periphery, B cells engage antigen through their BCR to become activated (Cyster and Allen,

2019). Activated B cells downregulate IgD surface expression and exchange their surface-bound IgM antibody with either IgG, IgA, or IgE isotypes through the process of isotype switching (Cyster and Allen, 2019). An antibody's isotype will determine its effector function. IgM antibodies are effective at activating complement (Cooper, 1985; Czajkowsky and Shao, 2009). IgG and IgA antibodies mediate protection against viruses and bacteria (Mond et al., 1995; Tyagi et al., 2023), and IgE antibodies confer protection against large extracellular parasites (Gould and Sutton, 2008). IgA is mostly produced within mucosal tissues, such as the gut and respiratory tract, whereas IgM, IgG, and IgE antibodies are generally released into the bloodstream (Brandtzaeg, 2007; Brandtzaeg, 2009). IgM antibodies are also large, existing as either pentamers or hexamers. In contrast, IgG and IgE exist as monomers, and IgA antibodies exist as dimers (Oostindie et al., 2022).

1.3 The Germinal Centre Response

Secondary lymphoid organs (SLOs), such the spleen and lymph nodes, are sites in which naïve B cells encounter antigen to initiate adaptive immune responses with help from T cells (Ruddle and Akirav, 2009). B cells and T cells are separated into two areas within SLOs: B cells cluster close to the periphery within so-called follicles, whereas T cells cluster near the centre of SLOs (Randall and Mebius, 2014; Ruddle and Akirav, 2009). The follicular region of SLOs also contain a network of follicular dendritic cells (FDCs). FDCs are specialized at retaining antigen on their surface in the form of immune complexes (ICs), which B cells can recognize (Heesters et al., 2014; Martínez-Riaño et al., 2023).

B cells bind antigen that has been captured on the surface of FDCs through their BCR (Nossal et al., 1964; Suzuki et al., 2009; Szakal et al., 1989). BCR engagement by cognate antigen

induces a cascade of signaling events that eventually result in the processing and presentation of antigen on major histocompatibility complex (MHC) class II molecules found on the surface of the B cell (Kwak et al., 2019). Following their activation, B cells upregulate the chemokine receptor, CCR7, to promote their migration to border between the T cell zone and B cell zone in SLOs (Okada et al., 2005; Reif et al., 2002). At the T-B border, B cells present peptide-MHC-II complexes to cognate $CD4^+$ helper T (T_H) cells. At this stage, B cells undergo rapid proliferation and can differentiate into memory B cells (MBCs) or into extrafollicular plasmablasts (PBs) that secrete low-affinity IgM antibodies to provide immediate immunological protection. Others will differentiate into germinal centre B (GCB) cells (Young and Brink, 2021).

Germinal centres (GCs) are highly specialized microanatomical structures that form in the B cell follicle of SLOs in response to infection or vaccination (Nieuwenhuis and Opstelten, 1984). These structures are typically transient, but they can exist chronically in mucosal tissues, notably the Peyer's patches in the intestine where B cells are constantly exposed to the gut microbiota and food antigens (Chen et al., 2020; Nowosad et al., 2020). Within GCs, antibodies undergo a secondary diversification process called somatic hypermutation (SHM) (Berek et al., 1991; Jacob et al., 1991). During SHM, GCB cells mutate the antigen-binding regions of their immunoglobulin genes as a means of generating mutants with enhanced antigen binding. Mutants with improved capacities for antigen binding undergo competitive expansion, whereas those with a diminished capacity for antigen binding are outcompeted. Through this Darwinian process of somatic diversification, GCB cells progressively generate antibodies with improved binding affinity. This phenomenon is called affinity maturation (Berek and Milstein, 1987; Eisen, 2014; Eisen and Siskind, 1964; Jerne, 1951). Affinity maturation is required to produce protective antibodies (Khurana et al., 2014; Tang et al., 2021; Verma et al., 2012). Indeed, sustained GC residency

permits high levels of SHM and endured affinity maturation, enabling the generation of broadly neutralizing antibodies against quickly evolving pathogens such as human immunodeficiency virus (Lee et al., 2022).

1.4 Germinal Centre Dynamics

Mature GCs are anatomically divided into two zones: a dark zone (DZ) and a light zone (LZ) (Nieuwenhuis and Opstelten, 1984). GCB cells move in a bi-directional manner between the DZ and LZ, with a net movement of GCB cells from the DZ into the LZ (Victora et al., 2010). Migration between the DZ and LZ is mediated by chemokines and the differential expression of chemokine receptors on GCB cells. GCB cells are retained in the DZ by the binding of CXCR4 to the chemokine, CCL12, which is produced by reticular stromal cells localized in the DZ. Conversely, LZ GCB cells express the CXCR5 chemokine receptor, which binds CXCL13 produced by FDCs residing in the LZ (Allen et al., 2004).

GCB cells residing in the DZ, called centroblasts, are highly proliferative and can be identified by high expression of CXCR4 (Allen et al., 2004; Gitlin et al., 2014; Victora et al., 2012; Victora et al., 2010). Within the DZ, GCB cells diversify their immunoglobulin genes by SHM (Weigert et al., 1970). SHM is initiated by activation-induced cytidine deaminase (AID), an enzyme specifically expressed in GCB cells (Muramatsu et al., 2000; Revy et al., 2000). AID deaminates deoxy-cytidine to deoxy-uracil within the immunoglobin variable region exon (Di Noia and Neuberger, 2007; Peled et al., 2008). Through its deamination activity, AID introduces U:G mismatches, which are fixed as point mutations within the immunoglobin variable regions once repaired. The mutations introduced by AID activity diversify antibody affinities and permit affinity-based selection, which occurs in the LZ. GCB cells in the LZ, called centrocytes, are

distinguished from centroblasts by high expression of the activation markers, CD83 and CD86, and low expression of CXCR4 (Victora et al., 2012; Victora et al., 2010). In the LZ, GCB cells encounter antigen displayed on the surface of FDCs in the form of ICs. Antigen retention on LZ FDCs is necessary for promoting the affinity and breadth of antibody responses (Kato et al., 2020; Martin et al., 2020; Martínez-Riaño et al., 2023). The LZ is also the site of positive selection. Here, the relative BCR affinities of GCB cells — which have undergone SHM in the DZ — are sensed by follicular T helper cells (T_{FH}), a specialized subset of $CD4^+$ T_H cells in the LZ (Victora and Nussenzweig, 2012). GCB cells that have acquired high-affinity mutations are selected by T_{FH} cells to re-enter the DZ, where they undergo clonal expansion and further rounds of SHM. T cell help is limiting for the LZ-to-DZ migration step: the loading of GCB cells with exogenous antigen — independently of BCR ligation — leads to their accumulation in the DZ (Victora et al., 2010). Thus, the cycling of GCB cells between proliferation and SHM in the DZ with affinity-based selection in the LZ underlies antibody affinity maturation.

The positive selection of GCB cells into the DZ, which permits additional rounds of SHM and proliferation, is known as cyclic re-entry. A defining feature of positively selected GCB cells is expression of the proto-oncogene, c-Myc (Dominguez-Sola et al., 2012). The c-Myc proto-oncogene is highly expressed in proliferating cells, with critical roles in ribosome biogenesis, DNA synthesis, and metabolism (Dong et al., 2020). Expression of c-Myc in B cells is necessary for GC formation and maintenance (Calado et al., 2012; Dominguez-Sola et al., 2012). In GCB cells, c-Myc expression is transient: c-Myc is only expressed within a small subset of LZ GCB cells, and as GCB cells move to the DZ, they lose c-Myc expression. The relative expression of c-Myc in GCB cells is also directly proportional to the amount of antigen they present to T_{FH} cells (Finkin et al., 2019). Moreover, the amount of c-Myc expressed in LZ GCB cells determines the number

of cell divisions they will undergo in the DZ. Indeed, the overexpression of c-Myc results in the accumulation of GCB cells in the DZ (Finkin et al., 2019). After entering the DZ, expression of the AP4 transcription factor — which is induced by c-Myc — will sustain c-Myc-dependent transcriptional programs once c-Myc expression is lost (Chou et al., 2016). Expression of *Ccnd3* in DZ GCB cells also upregulates expression of E2F transcription factors, promoting DNA replication and proliferation independently of c-Myc (Pae et al., 2021). Activation of mTORC1 signalling is another necessary step in cyclic re-entry (Ersching et al., 2017). Through mTORC1 signalling, GCB cells can increase biosynthesis of RNA, proteins and lipids, thereby increasing their overall anabolic capacity for rapid proliferation in the DZ.

Although T cells play an undeniable role in GC selection, they are not acutely limiting for the initiation of DZ re-entry in positively selected GCB cells. GCB cells haplo-insufficient for MHC-II (Yeh et al., 2018) or GCB cells with a deletion in the H2-O MHC-II chaperone (Draghi and Denzin, 2010) are not counter-selected during GC responses. The conditional deletion of MHC-II in GCB cells only modestly impairs S phase entry in LZ GCB cells (Long et al., 2022). Likewise, the depletion of T cells during on-going GC reactions does not halt cell cycle entry in LZ GCB cells. Experiments done by Long et al. (2022) suggest that T cells may instead drive the metabolic re-fueling of positively selected GCB cells, and hence their division capacity in the DZ, in an affinity-dependent manner, where high-affinity GCB cells undergo more re-fueling than low-affinity GCB cells. This model of GC selection suggests T cells can provide help to GCB cells with varying affinities, and ultimately, support clonally diverse immune responses against complex pathogens.

Aside from DZ re-entry, GCB cells receiving T cell help may also be instructed to exit the GC reaction and differentiate into memory B cells (MBCs) or antibody-secreting plasma cells

(PCs). Differentiation into MBCs involves the expression of a unique set of transcription factors, including *Hhex*, *Tle3* and *Bach2* (Laidlaw et al., 2020; Shinnakasu et al., 2016), with low-affinity GCB cells preferentially undergoing MBC differentiation (Shinnakasu et al., 2016; Smith et al., 1997; Viant et al., 2020). The differentiation of low-affinity GCB cells into MBCs is thought to expand the breadth of MBC reactivity towards secondary challenges. In contrast to MBC differentiation, high-affinity GCB cells are thought to preferentially undergo PC differentiation, which is induced by the transcription factors *Irf4, Prdm1,* and *Xbp1* (Kallies et al., 2007; Klein et al., 2006; Sciammas et al., 2006; Shaffer et al., 2004; Turner et al., 1994). This affinity-based model of PC differentiation arose from studies in mice carrying an anti-hen egg lysosome (HEL) transgene (Phan et al., 2006). In these mice, acquisition of a Y53D mutation within antigen-binding region of HEL-specific antibodies confers a 100-fold increase in antibody affinity, with both the GC and PC compartments quickly becoming enriched in high-affinity clones (Sprumont et al., 2023). In a polyclonal setting, PC differentiation is more permissive and occurs concurrently between both high- and low-affinity GCB cells to support diverse antibody responses (Sprumont et al., 2023; Sutton et al., 2024). At the transcriptional level, positively selected GCB cells destined for PC differentiation considerably overlap with GCB cells destined for DZ re-entry (ElTanbouly et al., 2024). Other than the induction of PC-defining genes in PC precursors, both populations upregulate *Myc* as well as *Myc* target genes, including cell cycle genes and the DZ surface marker, *Cxcr4*. The transcriptional similarities between GCB cells destined for DZ entry and PC differentiation might help support diverse antibody responses against quickly evolving pathogens such as Influenza.

The cytokines produced by T_{FH} cells help reinforce the molecular pathways dictating the choice between cyclic re-entry and GC exit. IL-4 and IL-21 are common gamma chain cytokines

produced by T_{FH} cells during GC responses. Production of IL-4 and IL-21 from T_{FH} cells is necessary for GC formation and affinity maturation (Chevrier et al., 2017; Gonzalez et al., 2018; Linterman et al., 2010; Zotos et al., 2010). IL-21-expressing T_{FH} cells are produced early during the GC response, and they gradually differentiate into IL-4-expressing T_{FH} cells as the GC response progresses (Weinstein et al., 2016). During positive selection, IL-21 synergizes with CD40 signalling to refuel positively selected GCB cells by upregulating c-Myc protein expression and the mTOR pathway (Luo et al., 2023). IL-21 signalling controls LZ-to-DZ cycling: deletion of the IL-21 receptor blocks S phase entry in LZ but not DZ GCB cells, and its deletion skews GCB cells towards a centrocyte phenotype (Zotos et al., 2021). In addition, IL-21 promotes the differentiation of $IRF4^{high}CD138^{+}$ PCs originating from the LZ (Luo et al., 2023). IL-4 similarly regulates GC dynamics and output. Limited IL-4 signalling in GCB cells is critical for ensuring efficient affinity maturation and MBC output. Increasing the bioavailability of IL-4 impairs affinity maturation and MBC differentiation in the LZ, while the deletion of either IL4Rα or STAT6 promotes MBC differentiation (Duan et al., 2021). IL-21 and IL-4 can also act synergistically to promote PC differentiation and GC formation (Weinstein et al., 2016).

1.5 Protein Arginine Methylation

Post-translational modifications (PTMs) have emerged as critical regulators of GC expansion and affinity maturation. PTMs are enzymatic modifications that involve the covalent addition of functional groups to proteins. These may include ubiquitination, phosphorylation, methylation, and acetylation. Key molecular regulators of the GC response, such as AID, undergo post-translational modifications to fine-tune their catalytic activity (McBride et al., 2006; McBride

et al., 2008). Post-translational modifications of histone proteins are also critical for controlling the gene networks governing GCB cell differentiation into MBCs and PCs (Wu et al., 2018).

In recent years, the epigenetic regulation of GC responses by protein methylation has received notable attention due to its relevance in GC-derived malignancies. *Ezh2* is a histone methyltransferase that catalyzes the H3K27me3 mark. This protein is highly expressed in DZ GCB cells and maintains their proliferative state via repression of the cell cycle checkpoint inhibitor, p21 (Béguelin et al., 2017). *Ezh2*$^{-/-}$ mice fail to form GCs due to heightened p21 activity, which represses E2F1-dependent transcription and S phase entry. Conversely, gain-of-function mutations in the *Ezh2* locus that increase its histone methyltransferase activity, such as Y164F, induce GC hyperplasia and promote the development of GC-derived lymphoma in mice (Béguelin et al., 2013; Béguelin et al., 2020). Loss of chromatin marks may also accelerate GC expansion. *Setd2* is histone methyltransferase that catalyzes the H3K36me3 chromatin mark. The heterozygous loss of *Setd2* in GCB cells — and hence the reduction in H3K36me3 levels on chromatin — increases GCB cell fitness and accelerates lymphomagenesis (Leung et al., 2022). *Setd2* heterozygous mutations are also highly recurrent in diffuse large B cell lymphoma (DLBCL) (Leung et al., 2022).

Protein arginine methylation is perhaps a less well studied but equally important PTM in GCB cells. This modification is mediated by protein arginine methyltransferases (PRMTs). There are nine members of the PRMT family. PRMTs catalyze the addition of methyl groups from S-adenosylmethionine to the terminal nitrogen atoms on the arginine side chain (Bedford and Clarke, 2009). Some PRMTs transfer only one methyl group, producing monomethylarginine (MMA) (Blanc and Richard, 2017). Others can add two methyl groups onto either the same nitrogen atom, producing asymmetric dimethylarginine (aDMA), or onto two different nitrogen atoms, producing symmetric dimethylarginine (sDMA) (Blanc and Richard, 2017). Type I PRMTs catalyze the

aDMA mark, while type II PRMTs catalyze the sDMA mark. The MMA mark is catalyzed by Type III PRMTs.

There is only one member of the PRMT family known to mediate the MMA mark: protein arginine methyltransferase 7 (PRMT7) (Blanc and Richard, 2017). PRMT7 catalyzes histone arginine methylation (Feng et al., 2013), notably the H4R3me1 mark, and its methyltransferase activity has been demonstrated to control splenic B cell development and GC expansion. The conditional deletion of *Prmt7* in B cells via the *Cd19*-cre driver induces GC hyperplasia due to increased *Bcl6* expression, the master transcription factor of the GC reaction. Conversely, *Prmt7* overexpression downregulates *Bcl6* expression and increases the H4R3me1 mark (Ying et al., 2015).

PRMT5 is a member of the Type II PRMT group with essential roles in B cell development and antibody responses (Blanc and Richard, 2017; Litzler et al., 2019). PRMT5 protects B cells from apoptosis during their development in the bone marrow as wells as following their activation in the periphery. The conditional deletion of *Prmt5* in Pro-B cells activates the p53-dependent apoptosis pathway and eliminates mature B cells from the spleen. PRMT5 is also required for the survival of activated B cells in immunized mice: *Prmt5* deficiency increases caspase activity following B cell activation. Furthermore, *Prmt5* deficiency in activated B cells significantly hampers GCB cell proliferation as well as antibody production and affinity maturation (Litzler et al., 2019). More recently, PRMT5 was shown to promote T_{FH} cell differentiation, and by extension B cell activation and GC formation (Read et al., 2024), highlighting its contribution to GC biology through B cell- and T cell-intrinsic mechanisms.

Type I PRMTs consist of six members, with PRMT1 being the primary mediator of the aDMA mark (Blanc and Richard, 2017; Tang et al., 2000). PRMT1 preferentially methylates

arginine amino acids within RCG/RG motifs and is responsible for over 90% of the arginine methylation in mammalian cells (Tang et al., 2000). PRMT1 has critical roles in cellular metabolism, DNA damage responses, proliferation, differentiation, and migration in diverse cell types (Blanc and Richard, 2017).

PRMT1 has pleiotropic functions in B cell development and effector responses. PRMT1 methylates the Igα subunit of the BCR complex at Arg198, negatively regulating BCR signalling (Infantino et al., 2010). Genetic ablation of the Arg198 methylation site increases the expression of adaptor proteins downstream of the BCR complex, notably Syk, and potentiates the release of intracellular Ca^{2+} ions in response to BCR ligation. Methylation of the Igα chain at Arg198 is also necessary for normal B cell development in the bone marrow and spleen (Infantino et al., 2010). Similarly, the genetic deletion of PRMT1 in B cells with the *Cd19*-cre driver impairs B cell development at the pre-B cell stage (Dolezal et al., 2017; Hata et al., 2016). In pre-B cells, PRMT1 methylates cyclin dependent kinase 4 (CDK4), blocking the formation of CDK4-CCND3 complexes to restrict pre-B cell proliferation and promote their differentiation (Dolezal et al., 2017). PRMT1 is also essential for GC formation and B cell proliferation. Deleting *Prmt1* in immature and transitional B cells with the *Cd23*-cre driver ablates GC formation and antibody production (Infantino et al., 2017). Furthermore, *Prmt1* deficiency in B cells reduces cell viability, increases apoptosis *ex vivo,* and dampens the expression of pro-survival genes such as *Bcl-2*, *Mcl-1* and *Bcl-x* (Infantino et al., 2017).

PRMT1 also controls GC dynamics and affinity maturation. During the GC reaction, *Prmt1* is upregulated in positively selected GCB cells destined for DZ re-entry through c-Myc- and mTOR-dependent pathways (Litzler et al., 2023). Using the *Cγ1*-cre driver (Casola et al., 2006), conditionally deleting *Prmt1* in activated B cells perturbs GC expansion (Litzler et al., 2023).

Prmt1-deficient GCB cells fail to progress normally through S phase, indicative of impaired DZ entry. Furthermore, they fail to accumulate sufficient affinity-maturing mutations in response to hapten-based immunizations compared to wild-type GCB cells. Consequently, affinity maturation is significantly impaired in *Prmt1*-deficient GCB cells, especially during recall responses. Interestingly, proportions of fate-mapped PCs are elevated in *Prmt1*$^{-/-}$ *Cγ1*-cre mice, and *ex vivo* activated *Prmt1*-deficient B cells readily differentiate into PCs and increase immunoglobulin secretion (Hata et al., 2016; Litzler et al., 2023). Proportions of MBC precursors and fate-mapped MBCs are similarly elevated in immunized *Prmt1*$^{-/-}$ *Cγ1*-cre mice, although *Prmt1*$^{-/-}$ *Cγ1*-cre mice fail to mount normal recall responses (Litzler et al., 2023). Taken together, these data demonstrate *Prmt1* prevents the premature exit of GCB cells into PCs to support continuous LZ-to-DZ cycling and affinity maturation.

1.6 Research Question and Aims

PRMT1 is highly expressed in leukemias, GC-derived lymphomas, such as GCB cell-like diffuse large B cell lymphoma (DLBCL), and across Hodgkin lymphoma (HL) cell lines (Leonard et al., 2012; Litzler et al., 2023). High PRMT1 expression is also correlated with poor patient survival in patients with DLBCL (Litzler et al., 2023), and elevated PRMT1-mediated arginine methylation in B cell lymphoma cells elevates expression of anti-apoptotic genes such as *Bcl2* (Goverdhan, 2017; Goverdhan et al., 2017). Similar to its role in GCB cells, the inhibition of PRMT1 in DLBCL cell lines also hinders cell growth and promotes PC differentiation (Goverdhan, 2017; Goverdhan et al., 2017; Litzler et al., 2023), and targeting PRMT1-mediated arginine methylation promotes anti-tumor immunity: Type I PRMT inhibition improves the efficacy of anti-PD1 blockade in numerous tumors models and is associated with an increased infiltration of

cytotoxic CD8+ T cells (Djajawi et al., 2024; Liu et al., 2023). As such, PRMT1 emerged as a promising target for the treatment of B cell lymphoma and other malignancies.

Unfortunately, a recent clinical trial reported limited therapeutic efficacy and significant toxicities in patients with advanced solid tumors and DLBCL after being given the Type I PRMT inhibitor, GSK3368715 (El-Khoueiry et al., 2023). Targeted degradation of PRMT1 has been proposed as an alternative strategy because it would require a much lower dose for inducing cancer cell death without causing significant toxicity (Martin et al., 2024). However, no successful attempts have been made. Heterogeneity in the trial's patient population, as well as the interplay between the different Type I and II PRMTs, could explain the poor therapeutic efficacy of GSK3368715 (El-Khoueiry et al., 2023). Indeed, there is redundancy in the substrates targeted by PRMTs. The inhibition of one PRMT protein can increase alternative arginine methylation patterns. For instance, downregulating *Prmt1* decreases Type I aDMA but increases Type II sDMA in some substrates (Dhar et al., 2013). Type I PRMT inhibition also more efficiently reduces tumor cell growth when combined with the genetic or pharmacological inhibition of Type II PRMTs (Fedoriw et al., 2019). Taken together, additional investigations of PRMT1-mediated arginine methylation in GCB cells and GC-derived malignancies are warranted.

Preliminary data from our lab also suggest that PRMT1 protein dosage dynamically controls GC expansion: while the homozygous deletion of *Prmt1* in activated B cells perturbs GC expansion, its heterozygous deletion caused an accumulation of GCB cells in the spleen following an acute immunization with sheep red blood cells (data not shown). Heterozygous deletions in histone modifiers or in proteins required for chromatin accessibility have been demonstrated to engender similar hypermorphic phenotypes in GCB cells. For instance, the complete deletion of the cohesion ATPase subunit, *Smc3,* hinders GC expansion, while its partial loss induces GC

hyperplasia and confers a cell-intrinsic fitness advantage due to heightened cell proliferation and reduced expression of GC-exit genes (Rivas et al., 2021). Similarly, the heterozygous loss of *Setd2* or *Smarac4* in activated B cells confer a cell-autonomous fitness advantage, both of which are linked to alterations in chromatic accessibility in GCB cells (Deng et al., 2024; Leung et al., 2022). Taken together, we hypothesize that the physiological expression of *Prmt1* in activated B cells limits GC formation and the antibody response. To test our hypothesis, we addressed the following research questions:

(1) How does the partial loss of *Prmt1* in activated B cells affect GC formation, GC polarity, and PC output?

(2) Is antibody production and/or affinity maturation elevated in *Prmt1*$^{+/-}$Cγ1-cre mice?

(3) How does *Prmt1* protein dosage in B cells intrinsically affect their proliferation, differentiation, and fitness?

Chapter II: Materials and Methods

Mice

Prmt1$^{f/f}$ mice (Yu et al., 2009), a gift from Dr. Stephen Richard (McGill University, Montréal, Canada), were bred with *Cγ1*-cre mice (Casola et al., 2006) to obtain *Prmt1*$^{+/+}$*Cγ1*$^{wt/cre}$ (Cγ1-cre), *Prmt1*$^{f/+}$*Cγ1*$^{wt/cre}$ (*Prmt1*$^{+/-}$Cγ1-cre), and *Prmt1*$^{f/f}$*Cγ1*$^{wt/cre}$ (*Prmt1*$^{-/-}$Cγ1-cre) mice. Mice were bred on the C57B/L6 background and housed in a specific pathogen-free plus (SPF+) facility at the Institut de Recherches Cliniques de Montréal (IRCM). All animal work was conducted following the guidelines of the Canadian Council for Animal Care and were approved by the IRCM animal protection committee (Protocol 2021-05).

Immunizations

To induce splenic germinal centre formation, 3- to 4-months-old mice were immunized by intraperitoneal injection (i.p.) with 100 ug of NP_{10}-CGG or NP_{13}-CGG (LCG Biosearch Technologies) at a 1:1 ratio with Imject Alum (Thermo Fisher Scientific). Male or female mice were used for all immunizations. Each experimental mouse was age- and sex-matched with a control mouse. Mice were bled and/or sacrificed 13 to 14 days post-immunization. Cγ1-cre or wild-type littermate mice were used as controls, as indicated in figure legends.

Induced-Germinal Centre B Cell (iGB) Cultures and Treatments

5-6 × 10^6 40LB feeder cells, a gift from Dr. Daisuke Kitamura (Tokyo University of Science, Tokyo, Japan (Nojima et al., 2011)), were treated with 10 ug/mL of mitomycin C (MMC) (BioShop, cat. #MIT232.10) in a 15cm dish for 1 hour at 37°C in DMEM media supplemented with 10% FBS (Wisent) and 1% penicillin/streptomycin (Wisent), hereafter referred to as complete

DMEM media. Complete DMEM media was supplemented with 10 mM HEPES (Wisent) during MMC treatments. Following mitomycin C treatment, 40LB were washed six times with PBS. For experiments in 24-well plates, arrested 40LB were plated at 0.15×10^6 cells per well in 0.5 mL complete DMEM media. For 10 cm dishes, 3×10^6 arrested 40LB were plated in 10 mL DMEM media. The following day, naïve B cells were purified from splenocytes using an EasySep Mouse B cell Isolation Kit (Stem Cell, cat. #19854) and magnet EasyEights (Stem Cell, cat. #18103), according to the instructions of the manufacturer. Three- to four-month-old, non-immunized mice were used for the purification of resting B cells. B cells were cultured at 37°C with 5% CO_2 in RPMI 1640 media (Wisent) supplemented with 10% FBS (Wisent), 1% penicillin/streptomycin (Wisent), 0.1 mM 2-mercaptoethanol (Bioshop), 10 mM HEPES (Wisent), 1 mM sodium pyruvate (Wisent), and 1 ng/ml IL-4 (PeproTech), hereafter referred to as complete iGB media. Naïve B cells were plated on arrested 40LB feeder cells at 0.02×10^6 B cells per 1 mL complete iGB media for 24-well plates, and for 10 cm dishes, 0.5 or 1.0×10^6 B cells in 10 mL complete iGB media were used. Cells were fed with complete iGB media at day 3 post-plating. Every day thereafter, fresh iGB media supplemented with 1 ng/ml IL-4 or 10 ng/mL IL-21 (PeproTech) was added after removing the top layer of media.

For experiments using the Type I PRMT inhibitor, MS023 (Cayman Chemical, cat. # 18361), naïve B cells were left on 40LB in complete iGB media for 24 hours, after they were treated were different dilutions of MS023 or DMSO for five days. MS023 stock was prepared at 50 mM in DMSO and stored at -80 °C. Working dilutions of MS023 were also prepared in DMSO and stored at -20 °C. Fresh working dilutions were prepared after two freeze/thaws. For the untreated controls, DMSO was added at a final concentration of 0.9%.

For competitive co-culture experiments, naive wild-type CD45.1 B cells were plated at a 1:1 ratio with naive Cγ1-cre, *Prmt1*$^{+/-}$ Cγ1-cre, or *Prmt1*$^{-/-}$ Cγ1-cre CD45.2 B cells on 40LB feeders. The frequency of CD45.2^{+} or CD45.1^{+} iGBs was calculated at day 6 post-plating after gating on total B220^{+} iGBs, B220^{+}CD38^{-}CD95^{+}GL7^{+} iGBs, or induced B220^{+}CD138^{+} plasmablasts.

For signalling experiments, iGBs were purified at day 4 by depleting 40LB feeders. First, iGBs and 40LB were detached with MACS buffer (PBS-BSA0.5%, 2 mM EDTA) and incubated with biotinylated anti-H2K (BioLegend, cat. #116303) at room temperature in MACS buffer. Then, the cell mixtures were incubated with anti-biotin microbeads (Miltenyi Biotec, cat. #130-105-637) and passed through LS columns (Miltenyi Biotec, cat. #130-042-401). Purified iGBs were obtained in the flow through and were allowed to rest for 1 hour at 37°C in iGB media before being stimulated with 10 ng/mL IL-21 (PeproTech).

Flow Cytometry

For the enumeration of splenocyte populations from NP-CGG immunized mice, spleens were mashed with a syringe plunge through a 70-um cell strainer in PBS-BSA1%. Splenocytes were re-suspended in 1 mL of red blood cell lysis buffer (155 mM NH4Cl, 10 mM KHCO3, 0.1 mM EDTA) and incubated at room temperature for 5 minutes. To stop the lysis reaction, splenocyte suspensions were washed with cold PBS. Then, splenocytes were re-suspended in 1 mL PBS-BSA1% and passed through a 40-um cell strainer. Splenocytes were counted using the Thermofisher Countess 3 Automated Cell Counter. Splenocytes were incubated with mouse FcR blocking antibodies (Miltenyi Biotec, cat. #130-092-575) for 10 minutes at 4°C prior to surface staining. Following FcR blocking, samples were stained with anti-B220, anti-CD4, anti-IgD, anti-

CD138, anti-CD95, anti-GL7, anti-CXCR4, anti-CD86, anti-CD44, anti-CD62L, anti-PD1, anti-CXCR5 antibodies, diluted in PBS-BSA1% for 30 minutes at 4°C. For intracellular stains, cells were fixed and permeabilized with the Foxp3/Transcription Factor Staining Buffer Set (Invitrogen, cat. #00-5523-00) overnight at 4°C and stained with the anti-Bcl6, anti-Foxp3, anti-IgM, or anti-IgG1 for 1 hour at 4°C in Invitrogen Wash/Perm Buffer. All antibodies used are listed in Table S1. To exclude dead cells in intracellular stains, samples were stained with eFluor780 fixable viability dye diluted 1:1000 in PBS (eBioscience, cat.#65-0865-14) prior to fixation/permeabilization. Otherwise, splenocytes were stained with 5 ug/mL 7-AAD (BioLegend, cat.#420404) for 30 minutes on ice before acquisition to gate on viable cells. Splenocyte samples were filtered through a 40-um cell strainer and acquired on the BD LSR Fortessa. All data were analyzed using FlowJo (BD Biosciences).

For staining iGBs, cells were detached with pre-warmed MACS buffer (PBS-BSA-0.5%, 2 mM EDTA) for 5 minutes at 37°C and counted manually or with the Thermofisher Countess 3 Automated Cell Counter. Prior to surface staining, iGBs were incubated with mouse FcR blocking antibodies (Miltenyi Biotec, cat. #130-092-575) for 10 minutes and stained with anti-B220, anti-CD138, anti-CD95, anti-CD38, anti-GL7, anti-IgG1, anti-IgM, anti-CD45.1, anti-CD45.2 antibodies listed in Table S1 for 30 minutes at 4°C. For detection of IRF4 in iGBs, cells were fixed and permeabilized with the Foxp3/Transcription Factor Staining Buffer Set for 1 hour at 4°C and stained with anti-IRF4 PE (Table S1). Here, samples were stained with eFluor506 fixable viability dye diluted 1:1000 in PBS (eBioscience, cat.#65-0866-14) before fixation/permeabilization. For detection of p-S6 in iGBs post-stimulation with IL-21, stimulated cells were fixed and permeabilized with BD Perm/Wash buffer (cat. #554723) supplemented with 1.5% formaldehyde at room temperature for 15 minutes and then on ice for 30 minutes, as described previously (Luo

et al., 2023). Following fixation/permeabilization, cells were blocked with mouse FcR blocking antibodies and stained overnight at 4°C with for anti-mouse pS6-PE (Table S1) in BD Perm/Wash buffer. As before, all acquisitions were performed on the BD LSR Fortessa and data were analyzed in FlowJo.

Enzyme-Linked Immunosorbent Assays (ELISAs)

Sandwich ELISAs were used to measure pre-immune sera antibody titers. For quantification of antibody titers in non-immunized mice, ELISA plates were coated with rat anti-mouse IgM, rat anti-mouse IgG1, rat anti-mouse IgG2b, or rat anti-mouse IgG3 (Table S1) in sodium carbonate-bicarbonate buffer. Antigen-specific antibody responses in immunized mice were assessed by direct or indirect ELISAs. Plates were coated with CGG (Biosearch Technologies), NP27-BSA (Biosearch Technologies), NP36-BSA (Biosearch Technologies), NP2-BSA (Biosearch Technologies) in carbonate-bicarbonate buffer, or with SARS-CoV-2 receptor binding domain (RBD) in PBS. For each coating, ELISA plates were incubated overnight at 4°C. Sera samples were then serially diluted and added to the coated plates and incubated overnight, followed by detection of total IgG, IgG1, IgG2b, IgG3, or IgM antibodies (Table S1). For detection of IgG1, IgG2b, IgG3 or IgM antibodies, plates were incubated with biotin rat anti-mouse IgG1, biotin rat anti-mouse IgG2b, biotin rat anti-mouse IgG3, or biotin rat anti-mouse IgM for 1 hour at 4°C with gentle shaking and then for another hour with Streptavidin-HRP (Table S1). For detection of IgG, plates were incubated with anti-mouse IgG conjugated to HRP for 1 hour at 4°C with gentle shaking (Table S1). After each incubation, plates were washed three times with PBS-Tween0.05%. Before plating read, HRP substrate was added to each well, and the plates were read at 405 nm on the SpectraMax 190 plate reader.

To measure antibody avidity, sera samples were diluted to obtain roughly similar working concentrations before being added to coated ELISA plates overnight at 4°C. Plates were washed three times with PBS-Tween0.05% before being incubated with increasing concentrations of Sodium Thiocyanate (Acros Organics) for 10 minutes at room temperature: 0, 0.05, 0.1, 0.25, 0.5, 1, 2, 2.5, 3, 3.5, 4, 5M. Plates were washed again three times with PBS-Tween0.05% and incubated with 0.1% gelatin for 10 minutes at room temperature. Specific antibody isotypes were then detected as described above. The relative avidities of antigen-specific antibodies were calculated as described previously (Deisenhammer et al., 1996; Zahn et al., 2013).

Western Blotting

Proteins were extracted from cell lysates with RIPA Buffer (150 mM NaCl, 1% NP-40, 0.5% Sodium Deoxycholate, 0.1% Sodium Dodelysulfate (SDS), 50 mM Tris-HCL pH = 7.4) with protease and phosphatase inhibitors (Thermofisher). Protein extracts were separated by SDS-PAGE and transferred onto a nitrocellulose membrane. Membranes were stained with Ponceau-S to control for equal loading and transfer of proteins. Next, membranes were blocked with TRIS-buffered saline (TBS) + 5% milk and incubated with the following primary antibodies in 5%BSA + 0.1%Tween20 + TBS overnight at 4°C: rat anti-mouse PRMT1 or rabbit anti-mouse Actin (Table S2). After incubation with the primary antibodies, membranes were washed three times in 5%BSA + 0.1%Tween20 + TBS for 5 minutes, followed by incubation with either anti-rat IgG Alexa 680 or anti-rabbit IgG IRDye 800CW secondary antibodies for 1 hour (Table S2). Membranes were washed again as before and visualized on the Odyssey CLx imaging system (LI-COR). ImageStudiolite software was used to quantify protein expression by normalizing the signal of the

protein of interest to the signal of the loading control. Original, uncropped images of Western blots are shown in supplementary Figure S5.

Statistics

All statistical analyses were performed using Graphpad Prism 10.0. Parametric statistical tests (i.e., Student's t-test or One-Way ANOVA) were only used for datasets that met the criteria for normality, following the Shapiro-Wilk test, with α set to 0.05. Otherwise, non-parametric tests (i.e., Mann-Whitney U test) were used. The test employed for each dataset is indicated in the figure legends. Only significant P-values (p<0.05) are shown.

Chapter III: Results

3.1 The partial loss of Prmt1 in activated B cells elevates proportions of splenic GCB cells

To explore the impact of *Prmt1* protein dosage on the humoral immune response, we crossed C57BL/6 mice carrying a floxed allele of the *Prmt1* gene with mice expressing the *Cγ1-Cre* recombinase, where Cre-mediated recombination occurs following T-cell mediated B cell activation (Casola et al., 2006). Upon reaching immunological maturity, $Prmt1^{+/+}C\gamma1^{wt/cre}$ (Cγ1-cre) and $Prmt1^{f/+}C\gamma1^{wt/cre}$ ($Prmt1^{+/-}$ Cγ1-cre) mice were immunized with 4-hydroxy-3-nitrophenylacetyl-chicken gamma globulin (NP-CGG) in Alum and sacrificed 13-14 days later, around the peak of the GC reaction to NP-CGG (Hannum et al., 2000). $Prmt1^{f/f}C\gamma1^{wt/cre}$ ($Prmt1^{-/-}$ Cγ1-cre) mice were also included as a control (**Fig 1A**). As expected, GCB cell frequencies and numbers were reduced in $Prmt1^{-/-}$ Cγ1-cre mice. Interestingly, immunized $Prmt1^{+/-}$ Cγ1-cre mice manifested a 2-fold increase in the frequency and number of GCB cells (**Fig 1B**). Spleen mass and total splenocyte counts were comparable across all three genotypes (**Fig S2A,B**), and there were no differences in the frequency or total number of $B220^+$ B cells or naïve IgD^+B220^+ B cells (**Fig 1C,D, S2C,D**).

Augmented GC responses are often accompanied by an impaired cycling of GCB cells between the DZ and LZ, resulting in the skewing of GC polarity (Deng et al., 2024; Leung et al., 2022; Rivas et al., 2021). We did not detect any change in the frequency of DZ or LZ GCB cells in $Prmt1^{+/-}$ Cγ1-cre mice (**Fig 1E**). Complete loss of *Prmt1* in GCB cells results in the accumulation of memory B cell precursors in the LZ, which can be identified by an increased frequency of $CXCR4^{low}CD86^{high}$ centrocytes among $IgD^{low}CD95^+$ GCB cells (Litzler et al., 2023). As expected, $CXCR4^{low}CD86^{high}CCR6^+$ memory B cell precursors were significantly elevated in $Prmt1^{-/-}$ Cγ1-cre mice. We noted a trend towards more memory B cell precursors in the GC LZ of

Prmt1$^{+/-}$ Cγ1-cre mice but overall, it was largely unaltered, suggesting pre-memory B cell development in the GC is functionally intact with the partial deletion of *Prmt1*, unlike in *Prmt1*$^{-/-}$ Cγ1-cre mice (**Fig 1F**).

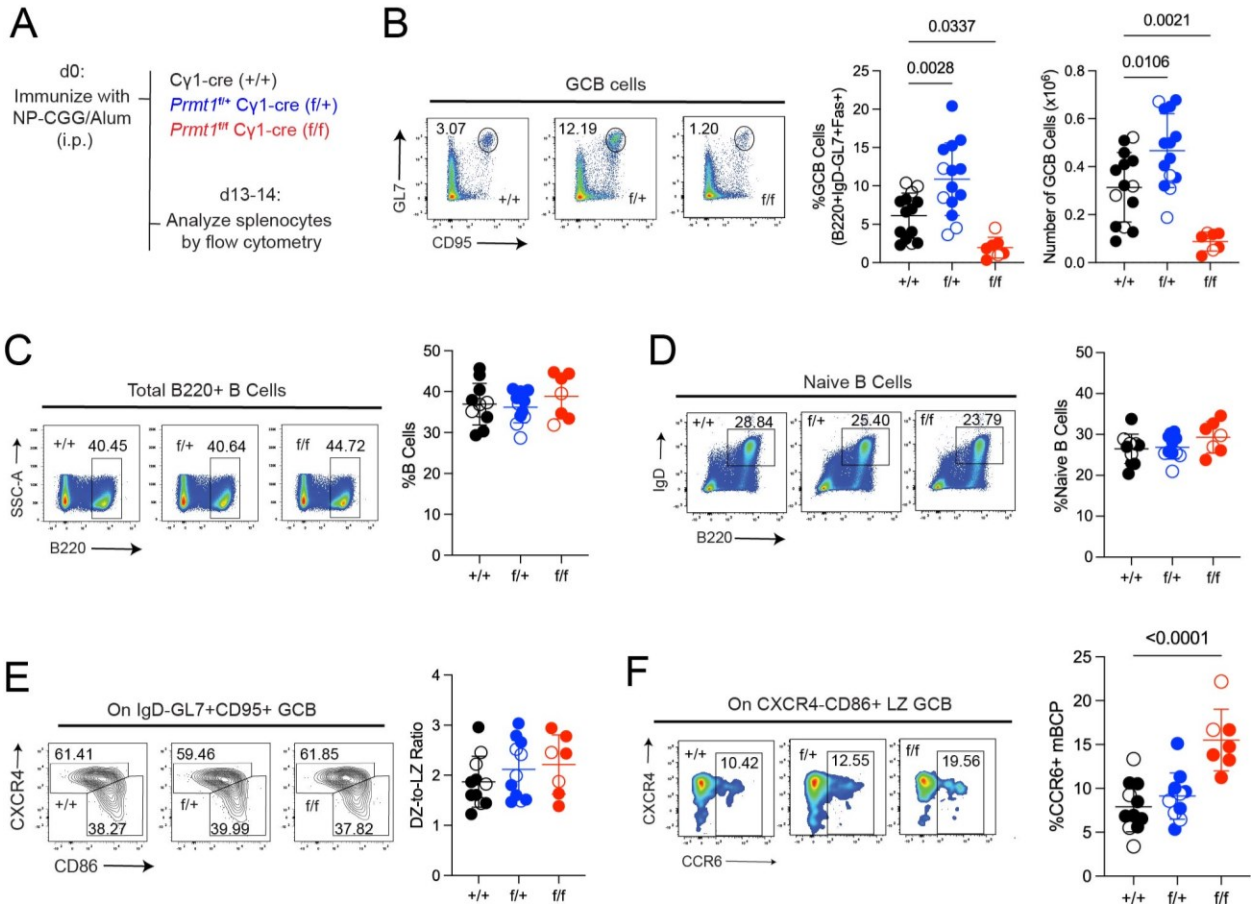

Figure 1. The monoallelic deletion of *Prmt1* in activated B cells increases frequencies of GCB cells in the spleen. (A) Experimental scheme for assessing splenic GCB cell responses in Cγ1-cre, *Prmt1*$^{+/-}$ Cγ1-cre, and *Prmt1*$^{-/-}$ Cγ1-cre using NP-CGG plus Alum. **(B)** Representative flow cytometry plots and pooled frequencies and numbers of splenic GCB cells (B220+IgD-GL7^{high}CD95^{high}) from Cγ1-cre, *Prmt1*$^{+/-}$ Cγ1-cre, and *Prmt1*$^{-/-}$ Cγ1-cre mice 13- or 14-days post-immunization with NP-CGG plus Alum. Data pooled from 2 to 4 independent experiments with 3 to 4 mice per genotype. **(C)** Representative flow cytometry plots and pooled frequencies of total splenic B220^{+} B cells from mice in (B). **(D)** Representative flow cytometry plots and pooled frequencies of naïve B220^{+}IgD^{+} B cells from mice in (B). **(E)** Representative flow cytometry plots and ratio of DZ-to-LZ GCB cells from mice in (B). **(F)** Representative flow cytometry plots and pooled frequencies of CXCR4^{low}CCR6^{+} memory B cell precursors from mice in (B). All error bars represent the mean ±SD. All P-values were calculated by One-Way ANOVA with Dunnett's multiple comparison test. Open circles represent male mice; closed circles are female mice.

T_{FH} cells are necessary for the formation and expansion of GCs. Thus, we set out to determine if the augmented GC frequency in *Prmt1*$^{+/-}$ Cγ1-cre mice was also accompanied by an elevated T_{FH} response. We did not detect any discernable differences in the frequency or total numbers of $CD4^+$ T cells in *Prmt1*$^{+/-}$ Cγ1-cre mice (**Fig S2E**), although we did observe a trend towards more activated $CD4^+CD62L^-CD44^+$ T cells (**Fig S2F**). Consistent with the elevated frequency of GCB cells in *Prmt1*$^{+/-}$ Cγ1-cre mice, there was a modest trend towards more $FOXP3^-$ $CXCR5^+PD1^+$ T follicular helper cells (**Fig S2G**). GCs also contain immunosuppressive $FOXP3^+$ T follicular regulatory (T_{FR}) cells that accumulate during the contraction phase of the GC response (Linterman et al., 2011; Merkenschlager et al., 2023). Unlike the T_{FH} response, frequencies and numbers of regulatory $FOXP3^+$ T_{FR} cells were unchanged (**Fig S2H)**, suggesting the elevated GCB cell frequency in *Prmt1*$^{+/-}$ Cγ1-cre mice did not arise from any breach in immunological tolerance.

Taken together, we demonstrate that *Prmt1* is not haplo-insufficient for the GC response. Furthermore, we find that the monoallelic and bi-allelic deletions of *Prmt1* in activated B cells have opposing effects on the GC response: whereas complete *Prmt1* deficiency impairs GC expansion, the heterozygous deletion of *Prmt1* in activated B cells elevates the frequency of splenic GCB cells in response to an acute immunization.

3.2 Antibody production and plasma cell differentiation are elevated in Prmt1$^{+/-}$ *Cγ1-cre mice*

The elevated GCB cell numbers in immunized *Prmt1*$^{+/-}$ Cγ1-cre mice prompted us to investigate whether the monoallelic deletion of *Prmt1* could similarly elevate antibody production. Because the antibody response in *Prmt1*$^{-/-}$ Cγ1-cre mice has been previously characterized (Litzler et al., 2023), we only focused on *Prmt1*$^{+/-}$ Cγ1-cre mice for subsequent analysis of the humoral immune response. In non-immunized *Prmt1*$^{+/-}$ Cγ1-cre mice, we observed a significant increase in

IgG1 and IgM titers and trends towards more IgG2b antibody production. IgG3 titres were also largely unchanged between Cγ1-cre and *Prmt1*$^{+/-}$ Cγ1-cre mice (**Fig 2A,B**).

Immunoglobulins produced at resting state would most likely be elicited against chronic environmental stimuli and may be influenced by the differential half-life and selection of each antibody isotype. Thus, we also set out to determine how the monoallelic deletion of *Prmt1* affects the antibody response during the acute immunization with NP-CGG plus Alum adjuvant (**Fig 2A**). NP-CGG plus Alum induces a T_H2-skewed immune response, with the preferential production of IgG1 antibodies. At day 13 or 14 post-immunization with NP-CGG, we quantified titres of total anti-NP IgG1 and high-affinity anti-NP_2 IgG1 in sera. Anti-NP IgG1 responses were similar between Cγ1-cre and *Prmt1*$^{+/-}$ Cγ1-cre mice (**Fig 2C**), suggesting the immune response against NP was largely unaltered, despite the increase in GCB cell numbers. However, in keeping with the elevated production of IgM antibodies at resting data, there was a significant increase in the production of total anti-NP IgM antibodies in immunized *Prmt1*$^{+/-}$ Cγ1-cre mice. High-affinity anti-NP_2 IgM antibodies — which would have been generated during the GC reaction — were also elevated (**Fig 2D**), but there was no change in the overall affinity of the anti-NP IgM response (**Fig 2E**). Likewise, the affinity of the anti-NP IgG1 response was unchanged (**Fig 2E**). Thus, whereas complete *Prmt1* deficiency impairs IgG1 antibody responses (Litzler et al., 2023), the partial loss of *Prmt1* in activated B cells elevates antigen-specific IgM antibody production without affecting the affinity maturation of anti-hapten antibodies.

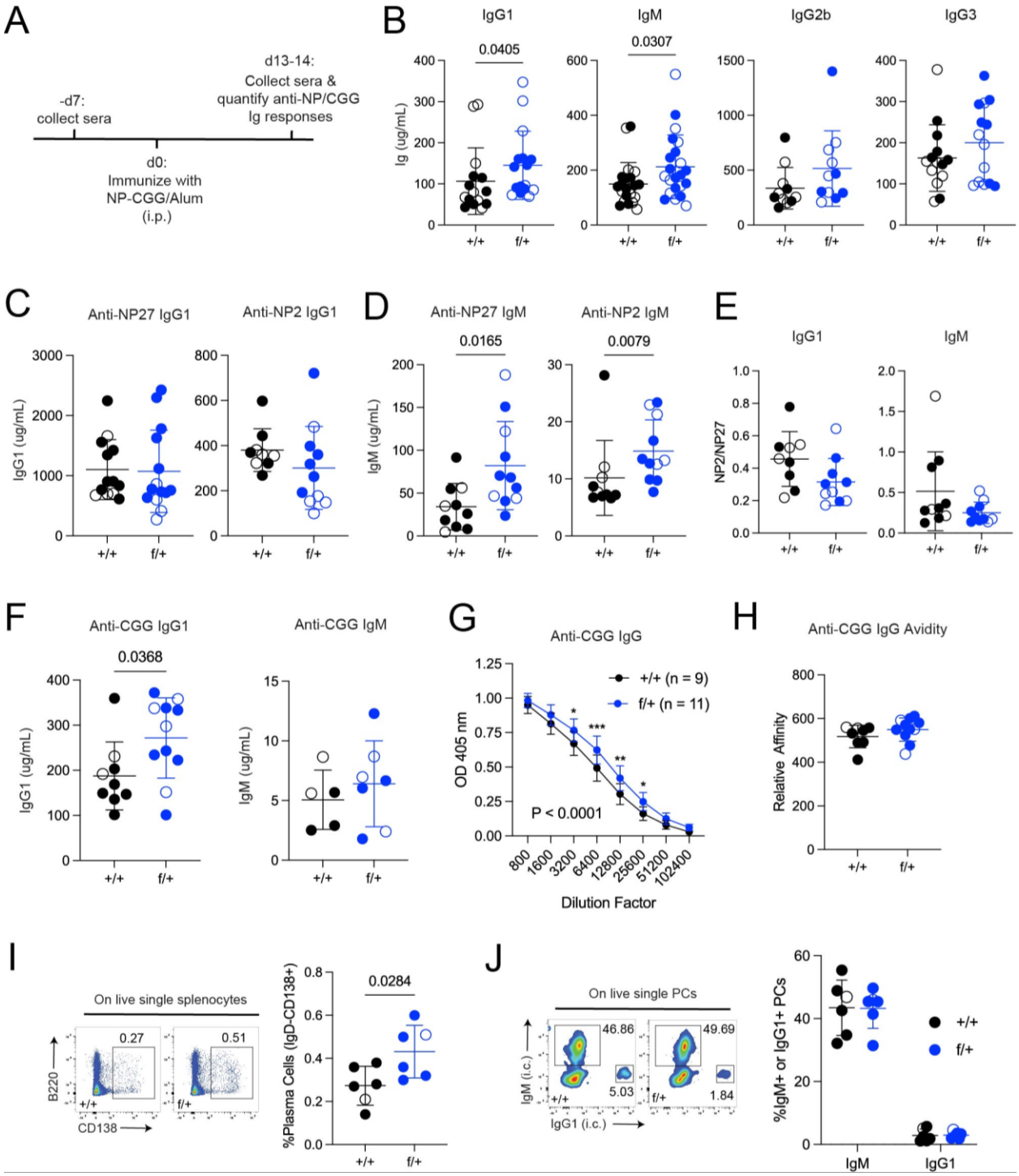

Figure 2. Antibody production and plasma cell frequencies are elevated in *Prmt1*$^{+/-}$ Cγ1-cre mice. (A) Experimental scheme for assessing anti-NP and anti-CGG antibody responses in *Prmt1*$^{+/-}$ Cγ1-cre using NP-CGG plus Alum. **(B)** Immunoglobulin titers from non-immunized control mice (Cγ1-cre or wild-type littermates) and *Prmt1*$^{+/-}$ Cγ1-cre mice. Data pooled from 3 to 5 independent experiments with 3 to 5 mice per genotype. P-values were calculated by Mann-Whitney U Test. **(C)** Quantification of total anti-NP27 IgG1 and high-affinity anti-NP2 IgG1 titers

in immunized control mice (Cγ1-cre n = 4-7 or wild-type littermates n = 6) and *Prmt1*$^{+/-}$ Cγ1-cre mice days 13 or 14 post-immunization with NP-CGG plus Alum. **(D)** Quantification of total anti-NP27 IgM and high-affinity anti-NP2 IgM titers in immunized control mice (Cγ1-cre n = 4 or wild-type littermates n = 6) and *Prmt1*$^{+/-}$ Cγ1-cre mice day 14 post-immunization with NP-CGG plus Alum. P-value was calculated by an unpaired Student's *t*-test for total anti-NP27 IgM titers, while the P-value was calculated by Mann-Whitney U Test for high-affinity anti-NP2 IgM. **(E)** Affinity maturation of the anti-NP IgG1 and anti-NP IgM responses from (C) and (D). Data in (C-E) are pooled from 3 to 4 independent experiments. **(F)** Titres of anti-CGG IgG1 or IgM antibodies at day 13 or 14 from Cγ1-cre and *Prmt1*$^{+/-}$ Cγ1-cre immunized with NP-CGG. P-value calculated by an unpaired Student's *t*-test. **(G)** Titres of anti-CGG IgG antibodies at day 13 or 14 from Cγ1-cre and *Prmt1*$^{+/-}$ Cγ1-cre immunized with NP-CGG. P-values calculated by Two-Way ANOVA with Šídák's multiple comparisons test. **p*<0.05, ***p* <0.01, ****p* <0.001. **(H)** Avidity of anti-CGG IgG antibodies at day 13 or 14 from Cγ1-cre and *Prmt1*$^{+/-}$ Cγ1-cre immunized with NP-CGG from mice in (G). Data in (F-H) are pooled from 3 independent experiments. **(I)** Representative flow cytometry plots and pooled proportions of splenic IgD^{-}CD138^{high} PCs from Cγ1-cre and *Prmt1*$^{+/-}$ Cγ1-cre mice day 14 post-immunization with NP-CGG. P-value was calculated by an unpaired Student's *t*-test. **(J)** Representative flow cytometry plots and pooled proportions of IgM^{+} and IgG1^{+} splenic PCs from (J). Data in (I-J) are pooled from two independent experiments. Opened circles represent male mice; closed circles are female mice.

Anti-NP antibody responses are clonally restricted, preferentially recruiting B cells expressing the IgHV1-72 heavy chain and Vλ1 light chain combination (Allen et al., 1988). In addition to the anti-NP antibody response, we also examined antibody production against the complex CGG carrier protein. CGG induces a polyclonal immune response, which might be more sensitive to affinity maturation defects. Anti-CGG IgM titres were unchanged in *Prmt1*$^{+/-}$ Cγ1-cre mice, but we did observe an increase in anti-CGG IgG1 and total anti-CGG IgG production (**Fig 3F, G**), suggesting *Prmt1*$^{+/-}$ Cγ1-cre mice manifest an enhanced polyclonal IgG antibody response. However, affinity maturation of the anti-CGG IgG response was unchanged (**Fig 3H**), like the anti-NP response.

In line with the elevated antibody production in *Prmt1*$^{+/-}$ Cγ1-cre mice, proportions of splenic PCs were also increased at day 14 post-immunization with NP-CGG (**Fig 2I**), but no change in the frequency of IgG1^{+} or IgM^{+} PCs was observed (**Fig 2J**). We confirmed the elevated polyclonal antibody response in *Prmt1*$^{+/-}$ Cγ1-cre mice using a Pfizer-like SARS-CoV-2 mRNA

vaccine — which induces an antibody response against the SARS-CoV-2 receptor binding domain (RBD) protein. At day 14, anti-RBD IgG titers were elevated in *Prmt1*$^{+/-}$ Cγ1-cre mice, mirroring the elevated anti-CGG IgG titres (**Fig S3E**). Importantly, the elevated antibody production in *Prmt1*$^{+/-}$ Cγ1-cre mice was restricted to the primary immune response: recall responses against NP-CGG or the SARS-CoV-2 mRNA vaccine were unchanged in *Prmt1*$^{+/-}$ Cγ1-cre mice (**Fig S3B, F**).

In summary, we find that the partial deficiency of *Prmt1* in activated B cells augments antibody production during the primary immune response, which can partly be explained by heightened PC output in *Prmt1*$^{+/-}$ Cγ1-cre mice. We also find no effect of *Prmt1* heterozygosity on affinity maturation, suggesting the monoallelic deletion of *Prmt1* does not affect GC dynamics, despite increasing frequencies of splenic GCB cells.

3.3 Prmt1 protein dosage restricts the fitness and differentiation of GCB cells and PCs

We next set out to determine whether the phenotypes in *Prmt1*$^{+/-}$ Cγ1-cre mice could be explained by intrinsic effects of *Prmt1* heterozygosity on B cell growth and differentiation. To that end, we cultured purified splenic B cells from Cγ1-cre, *Prmt1*$^{+/-}$ Cγ1-cre, and *Prmt1*$^{-/-}$ Cγ1-cre mice on 40LB fibroblasts expressing CD40 ligand (CD40L) and B-cell activating factor (BAFF) in the presence of the T cell-derived cytokine, interleukin-4 (IL-4). Together, these signals generate GC-like B cells *ex vivo*, called induced GCB cells or iGBs (Nojima et al., 2011).

When iGB expansion was scored over time, *Prmt1*$^{-/-}$ Cγ1-cre iGBs showed the expected growth defect at days 5 and 6, consistent with their previously reported proliferation defects (Litzler et al., 2023). However, there were no appreciable differences in cell growth or proliferation

between *Prmt1*$^{+/-}$ Cγ1-cre iGBs and Cγ1-cre iGBs (**Fig 3A, S4A**). Likewise, incorporation of EdU in GCB cells *in vivo* — which marks cells in S phase — revealed comparable levels of proliferating

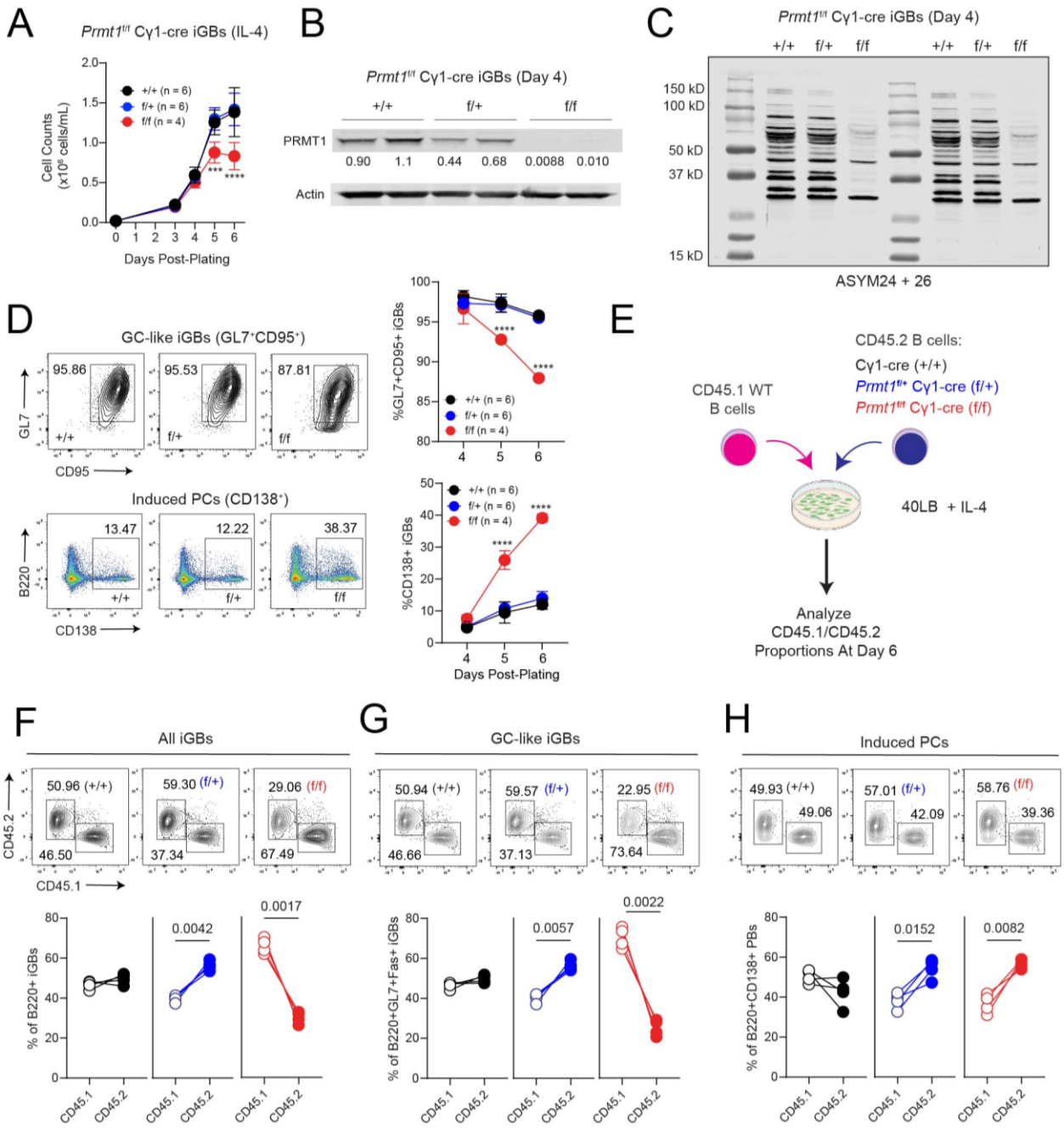

Figure 3. *Prmt1*$^{+/-}$ Cγ1-cre B cells have an intrinsic fitness advantage. (A) Cell counts of Cγ1-cre, *Prmt1*$^{+/-}$ Cγ1-cre, and *Prmt1*$^{-/-}$ Cγ1-cre iGBs grown with 1 ng/mL IL-4 from days 3 to 6 post-plating. Data are representative of three independent experiments, with each data point representing the mean ± SD. P-values were calculated by Two-Way ANOVA with Dunnett's multiple comparisons test. ***p<0.001, ****p<0.0001 **(B)** PRMT1 protein expression in Cγ1-cre,

Prmt1$^{+/-}$ Cγ1-cre, and *Prmt1*$^{-/-}$ Cγ1-cre iGBs at day 4, with the quantification of PRMT1 expression levels shown below. Actin was used as a loading control. **(C)** Western blot of asymmetrically di-methylated arginine in Cγ1-cre, *Prmt1*$^{+/-}$ Cγ1-cre, and *Prmt1*$^{-/-}$ Cγ1-cre iGBs at day 4. **(D)** Representative flow cytometry plots and pooled frequencies of GC-like iGBs (B220^{+}GL7^{+}CD38^{-} CD95^{+}) and PCs (B220^{+}CD138^{+}) between Cγ1-cre, *Prmt1*$^{+/-}$ Cγ1-cre, and *Prmt1*$^{-/-}$ Cγ1-cre iGBs from days 4 to 6 post-plating. Data are representative of three independent experiments, with each data point representing the mean ± SD. P-values were calculated by Two-Way ANOVA with Dunnett's multiple comparisons test, ****p<0.0001. **(E)** Experimental scheme for assessing the fitness of *Prmt1*$^{+/-}$ Cγ1-cre and *Prmt1*$^{-/-}$ Cγ1-cre iGBs. Image of fibroblasts was created with *BioRender*. **(F)** Representative flow cytometry plots and pooled frequencies of CD45.1^{+} and CD45.2^{+} iGBs, **(G)** CD45.1^{+} and CD45.2^{+} GC-like iGBs (B220^{+}GL7^{+}CD95^{+}), and **(H)** CD45.1^{+} and CD45.2^{+} PCs (CD138^{+}) at day 6. Data in (F-H) are pooled from four independent experiments. P-values in (F-H) were calculated by a paired *t*-test.

GCB cells between Cγ1-cre and *Prmt1*$^{+/-}$ Cγ1-cre mice (**Fig S4B**). Both PRMT1 protein and asymmetrically di-methylated arginine (ASYM) substrates were nearly absent in *Prmt1*$^{-/-}$ Cγ1-cre iGBs, which was consistent with PRMT1 being the primary mediator of the ASYM mark in mammalian cells (**Fig 3B,C**). In contrast, PRMT1 protein expression was reduced by about half in *Prmt1*$^{+/-}$ Cγ1-cre iGBs compared to Cγ1-cre iGBs at day 4, suggesting an efficient excision of the single *Prmt1* allele (**Fig 3B**). Examining the ASYM mark in *Prmt1*$^{+/-}$ Cγ1-cre iGBs revealed substrate-dependent differences with Cγ1-cre control iGBs (**Fig 3C**). Several bands showed no differences between Cγ1-cre and *Prmt1*$^{+/-}$ Cγ1-cre iGBs. However, ASYM was partially reduced in bands around the 50 kDa marker and was substantially depleted around the 100 kDa marker (**Fig 3C**).

In the iGB system, ~95% of iGBs acquire a GC-like phenotype (B220^{+}GL7^{+}CD95^{+}), with a small fraction of iGBs differentiating into PCs, marked by high expression of CD138. The percentage of GC-like iGBs was significantly reduced in *Prmt1*$^{-/-}$ Cγ1-cre iGBs but did not differ between Cγ1-cre and *Prmt1*$^{+/-}$ Cγ1-cre (**Fig 3D**). Similarly, the proportion of CD138^{+} PCs were increase with complete *Prmt1* deficiency, as described previously (Litzler et al., 2023), but did not differ between Cγ1-cre and *Prmt1*$^{+/-}$ Cγ1-cre cultures (**Fig 3D**). Accordingly, protein expression of

IRF4 — a transcription factor necessary for PC differentiation (Klein et al., 2006) — was significantly elevated in *Prmt1*$^{-/-}$ Cγ1-cre iGBs, but this was not the case for *Prmt1*$^{+/-}$ Cγ1-cre iGBs (**Fig 5SD**). Thus, *Prmt1* is not haplo-insufficient to support GCB cell proliferation, nor for the acquisition of GC or PC phenotypes *ex vivo*.

Prmt1 expression in GCB cells directly opposes the PC program, and the inhibition of Type I PRMT arginine methylation increases PC differentiation in a dose-dependent manner (Litzler et al., 2023). Thus, we were surprised to find no obvious alteration in PC differentiation with half the dose of *Prmt1*, especially since splenic PC frequencies were increased in immunized *Prmt1*$^{+/-}$ Cγ1-cre mice. While the reduction in asymmetrically methylated arginine in *Prmt1*$^{+/-}$ Cγ1-cre iGBs was insufficient to promote PC differentiation, we speculated that it would at least be sufficient to poise *Prmt1*$^{+/-}$ Cγ1-cre iGBs towards the PC program. To that end, we treated Cγ1-cre and *Prmt1*$^{+/-}$ Cγ1-cre iGBs with increasing doses of a Type I PRMT inhibitor (MS023) and analyzed the frequency of PCs after five days of treatment. Treating *Prmt1*$^{+/-}$ Cγ1-cre iGBs with MS023 increased proportions of IRF4^{high}CD138^{+} iGBs to a much greater extent than treated Cγ1-cre iGBs (**Fig S5F,G**). Furthermore, MS023 treatment significantly enhanced IRF4 expression among CD138^{-} *Prmt1*$^{+/-}$ Cγ1-cre iGBs but not CD138^{-} Cγ1-cre iGBs — analogous to the augmented IRF4 protein expression in CD138^{-} *Prmt1*$^{-/-}$ Cγ1-cre iGBs (**Fig S5H**). Thus, half the dose of *Prmt1* is sufficient to poise B cells towards the PC fate but insufficient to measurably augment PC differentiation *ex vivo*.

Although *Prmt1*$^{+/-}$ Cγ1-cre iGBs did not manifest any obvious alterations in proliferation and PC differentiation, this did not rule out selective advantages of partially deleting *Prmt1* in B cells. Thus, we next set out to directly test the fitness of *Prmt1*$^{+/-}$ Cγ1-cre B cells. To that end, we cocultured naïve CD45.1^{+} wild-type B cells with either naïve CD45.2^{+} Cγ1-cre, *Prmt1*$^{+/-}$ Cγ1-cre,

or *Prmt1*$^{-/-}$ Cγ1-cre B cells at a 1:1 ratio on 40LB feeders supplemented with IL-4 and assessed their competitive growth at day 6 post-plating (**Fig 3E**). CD45.2^{+} *Prmt1*$^{-/-}$ Cγ1-cre iGBs were significantly out-competed by CD45.1^{+} wild-type iGBs at day 6 (**Fig 3F**). In contrast, CD45.2^{+} *Prmt1*$^{+/-}$ Cγ1-cre iGBs significantly out-competed the CD45.1^{+} WT iGBs (**Fig 3F**), indicating the partial loss of *Prmt1* in activated B cells confers a cell-intrinsic fitness advantage.

Given both GCB and PC compartments were elevated in immunized *Prmt1*$^{+/-}$ Cγ1-cre mice, we wondered if the fitness advantage of *Prmt1*$^{+/-}$ Cγ1-cre B cells would extend to both GC-like iGBs and PC populations. We, therefore, determined proportions of CD45.2^{+} and CD45.1^{+} cells among B220^{+}GL7^{+}CD95^{+} GC-like iGBs and CD138^{+} PCs. *Prmt1*$^{+/-}$ Cγ1-cre GC-like iGBs overtook their WT competitors, while *Prmt1*$^{-/-}$ Cγ1-cre GC-like iGBs were significantly outcompeted (**Fig 4G**). In the case of PCs, both *Prmt1*$^{+/-}$ and *Prmt1*$^{-/-}$ Cγ1-cre PCs out-competed the WT PCs at day 6 (**Fig 4H**). Full *Prmt1* deficiency significantly elevated frequencies of CD45.2^{+}CD138^{+} PCs (**Fig S4E**), as expected (Litzler et al., 2023). However, there was no difference in the frequency of PCs between CD45.2^{+} *Prmt1*$^{+/-}$ Cγ1-cre and CD45.1^{+} WT iGBs (**Fig S4E**), indicating that *Prmt1* heterozygosity augments the fitness of PCs rather than expediting PC differentiation.

In short, the monoallelic deletion of *Prmt1* in B cells post-activation confers a cell-autonomous fitness advantage.

3.4 IL-4 and IL-21 differentially control the fitness of Prmt1$^{+/-}$ *Cγ1-cre and Prmt1*$^{-/-}$ *Cγ1-cre iGBs*

In the LZ, GCB cells respond to IL-4 and IL-21 produced by T_{FH} cells (Weinstein et al., 2016). Furthermore, they receive activation signals through BCR ligation to protect themselves from apoptosis (Chen et al., 2023). PRMT1 methylates STAT proteins, notably STAT1 and STAT3

(Djajawi et al., 2024; Sen et al., 2018; Yang et al., 2022), which act downstream of IL-4 and IL-21 in B cells, in addition to playing a critical role in dampening BCR signal transduction (Infantino et al., 2010; Infantino et al., 2017). However, our *ex vivo* investigations of *Prmt1*$^{+/-}$ Cγ1-cre B cells so far relied only on IL-4 and anti-CD40 stimulations. Thus, we set out to explore the growth and fitness of *Prmt1*$^{+/-}$ Cγ1-cre B cells grown with IL-21 or BCR stimulation, both equally important activation signals for GCB cells. By doing so, we reasoned we would be able to identify the signalling pathways altered in B cells with half the dose of PRMT1, as done previously in other systems (Enterina et al., 2022; Meyer et al., 2021).

The addition of agonist anti-IgM and anti-IgG antibodies to *Prmt1*$^{+/-}$ Cγ1-cre iGBs did not significantly alter cell growth compared to stimulated Cγ1-cre iGBs (**Fig S6B**), nor did we observe any effect on their differentiation. However, BCR stimulation in *Prmt1*$^{-/-}$ Cγ1-cre iGBs did augment PC differentiation and impair their competitive fitness (**Fig S6B,C,D,E**). We could also not detect any difference in the competitive fitness of *Prmt1*$^{+/-}$ Cγ1-cre iGBs grown with or without BCR stimulation (**Fig S6E**). Overall, the monoallelic deletion of *Prmt1* does not render B cells more sensitive to BCR-induced activation, unlike *Prmt1* complete deficiency.

IL-21 induces Bim-dependent apoptosis when given to naïve B cells directly (Jin et al., 2004; Mehta et al., 2003). Therefore, to monitor the effects of IL-21 on *Prmt1*$^{+/-}$ Cγ1-cre B cells, we first plated naïve Cγ1-cre, *Prmt1*$^{+/-}$ Cγ1-cre, and *Prmt1*$^{-/-}$ Cγ1-cre B cells on 40LB fibroblasts with IL-4 but switched IL-4 with IL-21 at day 3 post-plating, continuously adding IL-21 to the culture up until day 6. In line with the synergistic effects of IL-21 and IL-4 on GCB cell proliferation (Nojima et al., 2011; Weinstein et al., 2016), adding IL-21 to the culture accelerated iGB proliferation, as assessed by CTV staining (**Fig S2A**). As with the IL-4 cultures, Cγ1-cre and *Prmt1*$^{+/-}$ Cγ1-cre iGBs also grew at a comparable rate (**Fig 4A**). However, the addition of IL-21 to

the co-culture significantly enhanced the fitness advantage of GC-like *Prmt1*$^{+/-}$ Cγ1-cre iGBs compared to IL-4 alone (**Fig 4B-F**). Interestingly, *Prmt1*$^{-/-}$ Cγ1-cre iGBs did not manifest a growth defect with IL-21, and the fitness defect observed among all CD45.2^{+} *Prmt1*$^{-/-}$ Cγ1-cre iGBs in the IL-4 cultures was lost after the addition of IL-21. However, discriminating GC-like iGBs from PCs revealed that this apparent rescue arose from differential sensitivities of these two populations: GC-like *Prmt1*$^{-/-}$ Cγ1-cre iGBs showed a modest fitness disadvantage, while the corresponding PCs drastically overtook their WT competitors (**Fig 4B-E**). The competitive fitness of *Prmt1*$^{-/-}$ Cγ1-cre PCs in the IL-21 cultures was also increased compared to the IL-4 co-cultures (**Fig 4F**), despite IL-4 induces greater levels of PC differentiation, indicating IL-21 elevates PC fitness in *Prmt1*$^{-/-}$ Cγ1-cre iGBs to a much greater extent than IL-4.

In naïve B cells and GCB cells, IL-21 activates the PI3K/AKT/mTOR pathway (Dvorscek et al., 2022; Zotos et al., 2021), which is a critical regulator of cell metabolism, growth, and survival (Glaviano et al., 2023; Luo et al., 2023; Panwar et al., 2023). We postulated that the fitness of *Prmt1*$^{+/-}$ Cγ1-cre iGBs may be enhanced by IL-21 through augmented PI3K/AKT/mTOR activation. To that end, we grew iGBs with IL-4 until day 4, at which point we purified the iGBs from the 40LB feeders, allowed them rest, and then stimulated them with IL-21. As a read-out for mTOR activation, we analyzed protein expression of phosphorylated ribosomal S6 (p-S6), which is a downstream substrate of the PI3K/AKT/mTOR pathway and is often used a marker for mTOR activation (Ma and Blenis, 2009; Yang et al., 2014). At 2 hours post-stimulation, protein expression of p-S6 was significantly elevated in *Prmt1*$^{+/-}$ Cγ1-cre iGBs and to a lesser extent in *Prmt1*$^{-/-}$ Cγ1-cre iGBs (**Fig 4G**).

We conclude that *Prmt1* differentially interacts with IL-4 and IL-21 cytokine signalling to restrict the differentiation and fitness of GCB cells and PCs.

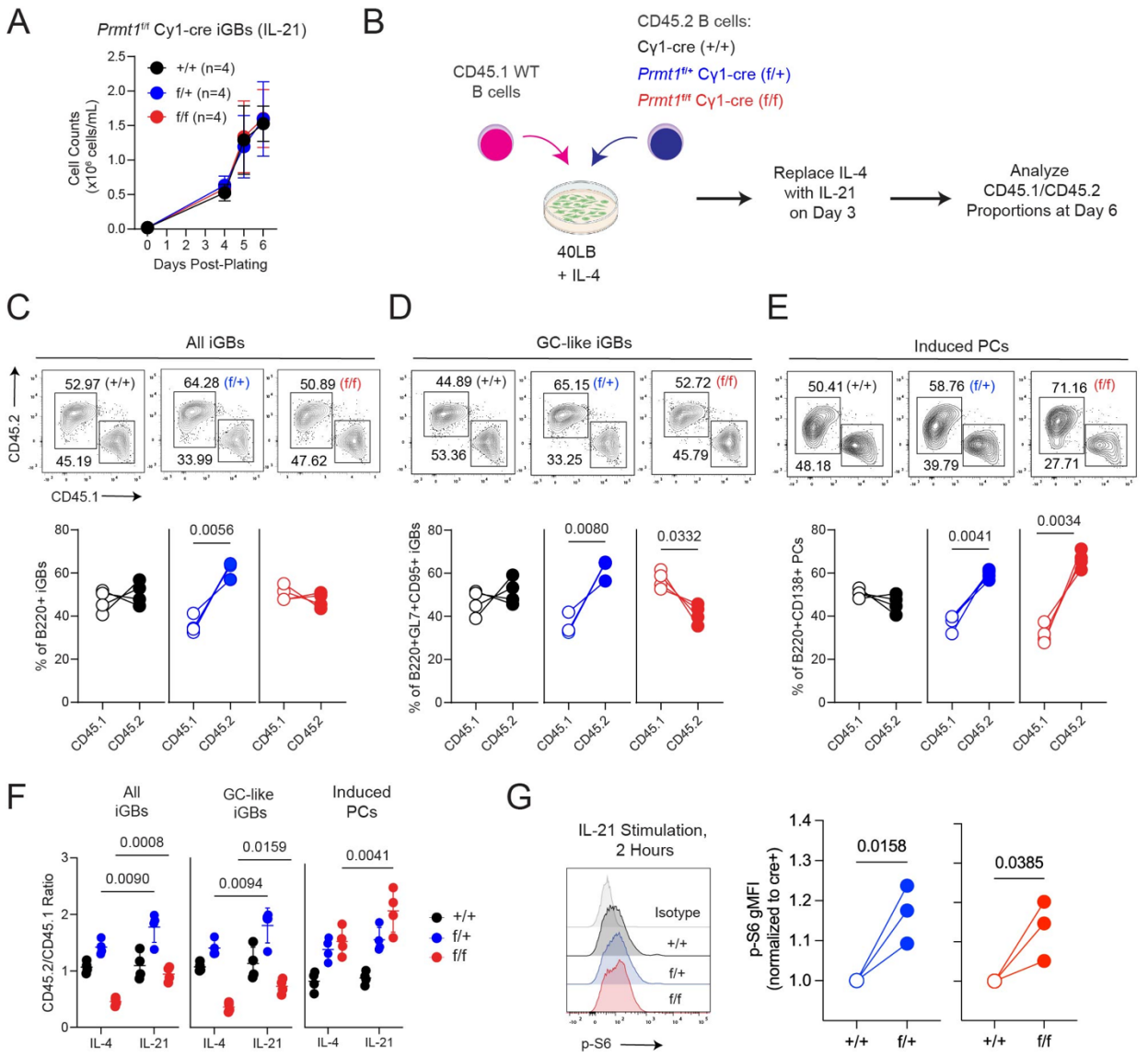

Figure 4. IL-21 augments the fitness of *Prmt1*$^{+/-}$ Cγ1-cre B cells. (A) Cell counts of Cγ1-cre, *Prmt1*$^{+/-}$ Cγ1-cre, and *Prmt1*$^{-/-}$ Cγ1-cre iGBs grown with IL-21 from days 4 to 6 post-plating. Data are representative of three independent experiments, with each data point representing the mean ± SD. **(B)** Experimental scheme for assessing the competitive fitness of iGBs grown with IL-21. Image of fibroblasts was created with *BioRender*. **(C)** Representative flow cytometry plots and pooled frequencies of CD45.1^{+} and CD45.2^{+} iGBs, **(D)** GC-like iGBs (B220^{+}GL7^{+}CD38^{-}CD95^{+}), and **(E)** PCs (B220^{+}CD138^{+}) between Cγ1-cre, *Prmt1*$^{+/-}$ Cγ1-cre, and *Prmt1*$^{-/-}$ Cγ1-cre iGBs at day 6. Data in (C-E) are representative of four independent experiments. P-values in (C-E) were calculated by a paired *t*-test. **(F)** Ratios of CD45.2^{+} to CD45.1^{+} iGBs between IL-4 and IL-21 cultures. P-values calculated by Two-Way ANOVA with Šídák's multiple comparisons test. **(G)** Normalized protein expression of p-S6 (geometric mean fluorescence intensity) in *Prmt1*$^{+/-}$ Cγ1-cre and *Prmt1*$^{-/-}$ Cγ1-cre iGBs stimulated with 10 ng/mL IL-21 for 2 hours. Data pooled from three independent experiments. P-values calculated by unpaired Student's *t*-test.

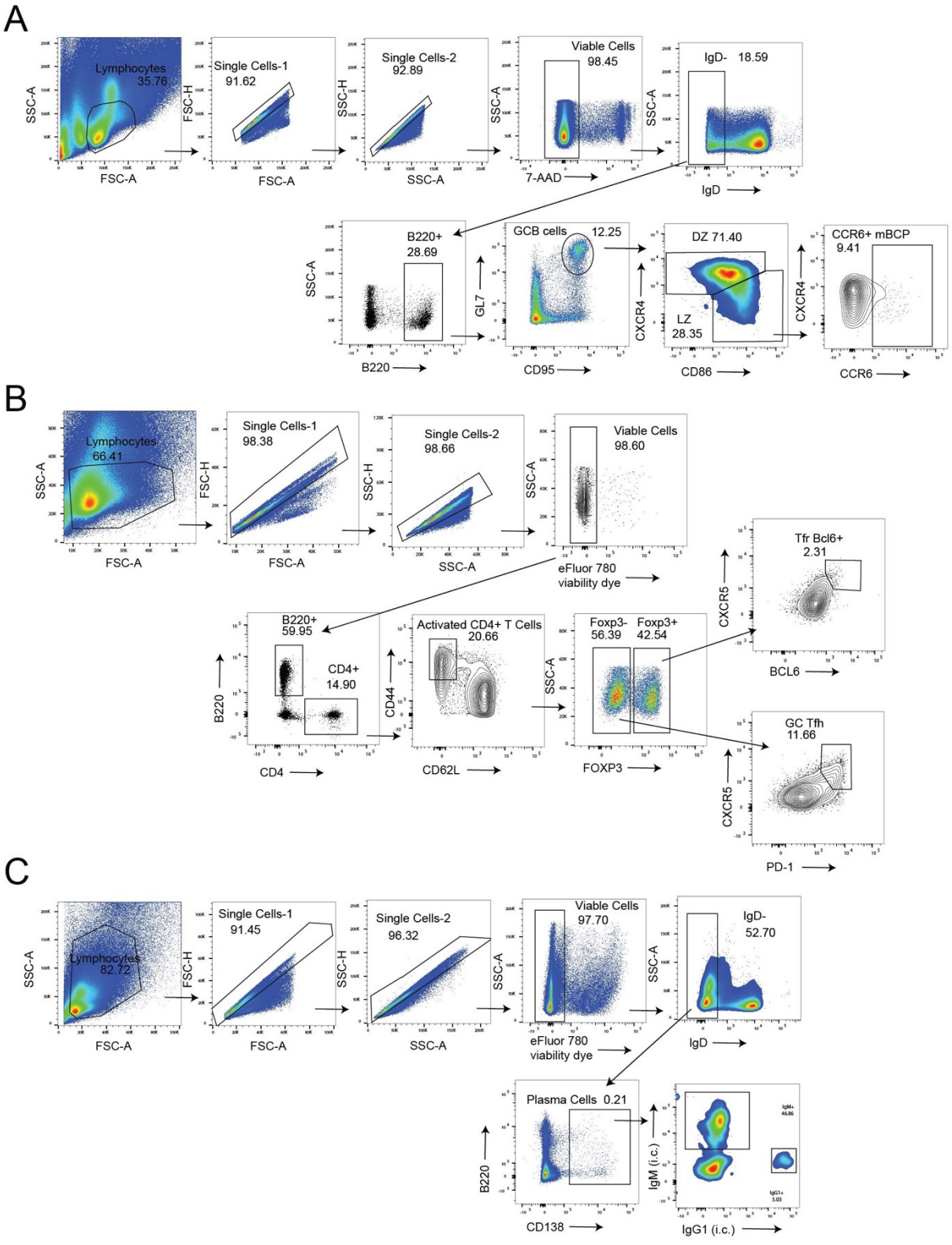

Supplementary Figure 1. Flow cytometry gating strategies for assessing frequencies of splenic GCB cells, T_{FH} and T_{FR} cells, and PCs. (A) Gating strategy for enumerating frequencies of GCB cells, DZ and LZ GCB cells, as well as LZ memory B cell precursors. **(B)** Gating strategy

for enumerating frequencies of splenic T_{FH} and T_{FR} cells. **(C)** Gating strategy for enumerating frequencies of total splenic PCs, IgG1+ PCs, and IgM+ PCs.

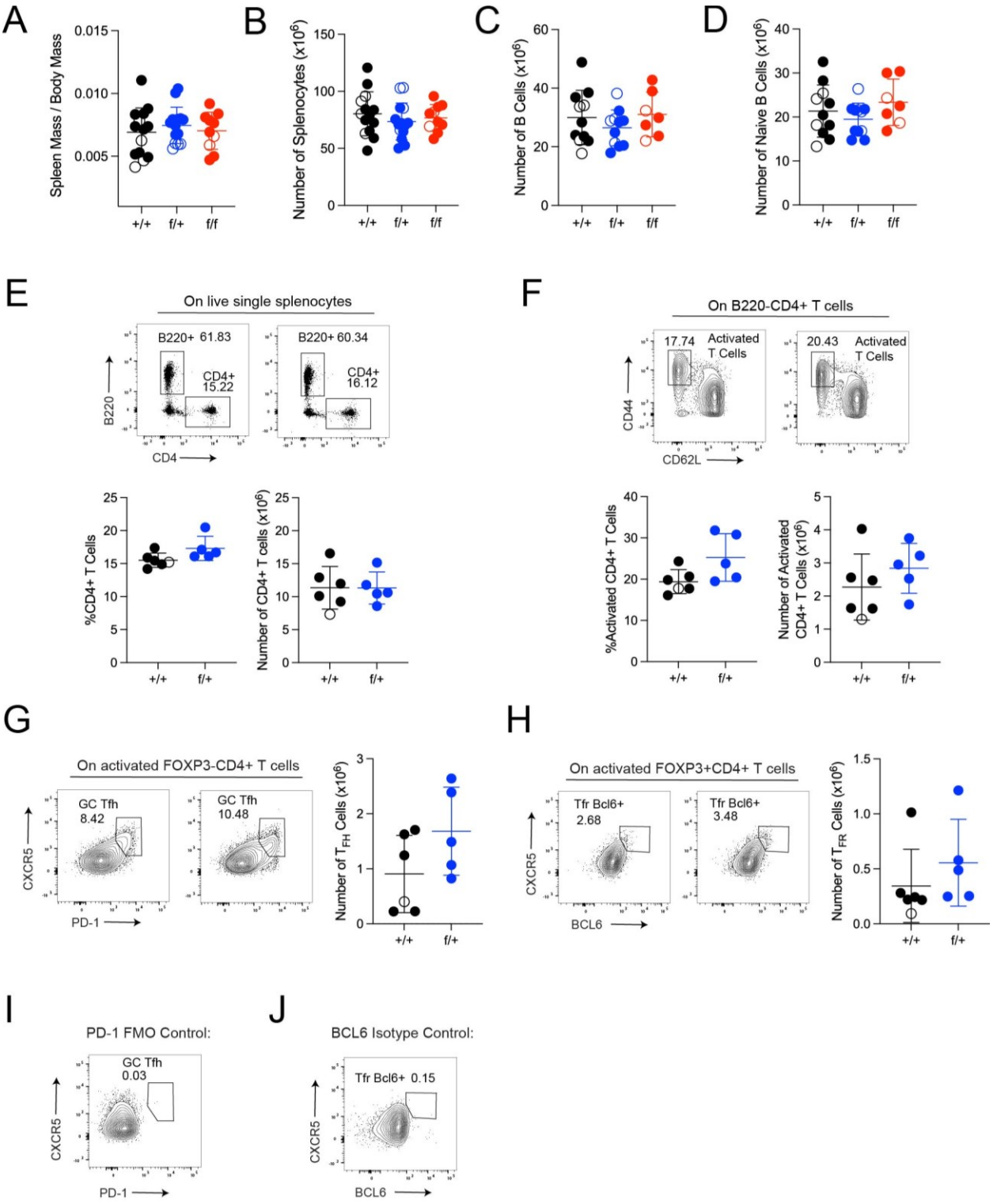

Supplementary Figure 2. Splenic B cell and T cell populations in immunized *Prmt1*$^{+/-}$ Cγ1-cre mice. (A) Spleen-to-body mass ratio of Cγ1-cre, *Prmt1*$^{+/-}$ Cγ1-cre, and *Prmt1*$^{-/-}$ Cγ1-cre mice day 13 or 14 post-immunization with NP-CGG. **(B)** Total splenocyte counts from mice in (A). **(C)** Numbers of splenic B220^{+} B cells and **(D)** numbers of naïve IgD^{+}B220^{+} B cells from Cγ1-cre, *Prmt1*$^{+/-}$ Cγ1-cre, and *Prmt1*$^{-/-}$ Cγ1-cre mice day 13 or 14 post-immunization with NP-CGG**. (E)** Representative flow cytometry plots and pooled frequencies and numbers of splenic B220^{-}CD4^{+} T cells from Cγ1-cre and *Prmt1*$^{+/-}$ Cγ1-cre mice at day 14 post-immunization with NP-CGG. **(F)** Representative flow cytometry plots and pooled frequencies and numbers of activated CD4^{+} T cells from mice in (E). **(G)** Representative flow cytometry plots and pooled numbers of CD4^{+}FOXP3^{-} T_{FH} cells from mice in (E). **(H)** Representative flow cytometry plots and pooled numbers of CD4^{+}FOXP3^{+} T_{FR} cells from mice in (E). **(I)** Representative flow cytometry plot for the PD-1 fluorescence minus one control, used to gate on CD4^{+}FOXP3^{-} T_{FH} cells. **(J)** Representative flow cytometry plot for the BCL6 BV421 isotype control, used to gate on CD4^{+}FOXP3^{+} T_{FR} cells. Data in (E-H) were pooled from 2 independent experiments, with 3 mice per genotype. Opened circles represent male mice; closed circles are female mice.

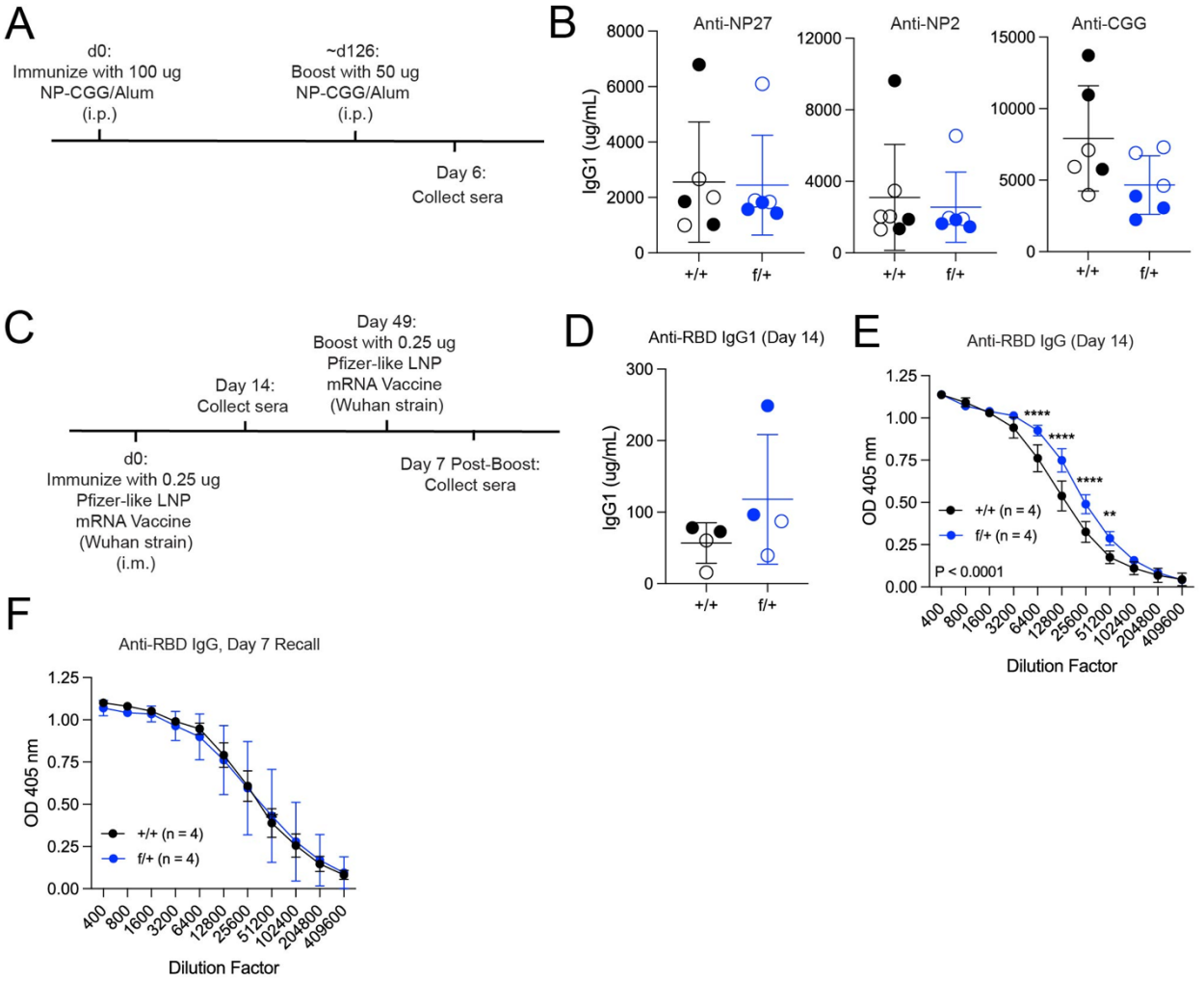

Supplementary Figure 3. Memory responses are intact in *Prmt1*$^{+/-}$ Cγ1-cre mice. (A) Prime and boost strategy for assessing memory responses in Cγ1-cre and *Prmt1*$^{+/-}$ Cγ1-cre mice using NP-CGG. **(B)** Quantification of anti-NP27, anti-NP2, and anti-CGG IgG1 titers 6 days post-boost. Data pooled from two independent experiments, with 3-5 mice per genotype. **(C)** Prime and boost strategy for assessing memory responses in Cγ1-cre and *Prmt1*$^{+/-}$ Cγ1-cre mice using a Pfizer-like SARS-CoV-2 mRNA vaccine. **(D)** Quantification of anti-RBD IgG1 titers and **(E)** anti-RBD IgG titers day 14 post-immunization with the Pfizer-like SARS-CoV-2 mRNA vaccine from one experiment. **(F)** Anti-RBD IgG titers 7 days post-boost in Cγ1-cre and *Prmt1*$^{+/-}$ Cγ1-cre mice. Data in (D-F) are from one experiment. Opened circles represent male mice; closed circles are female mice.

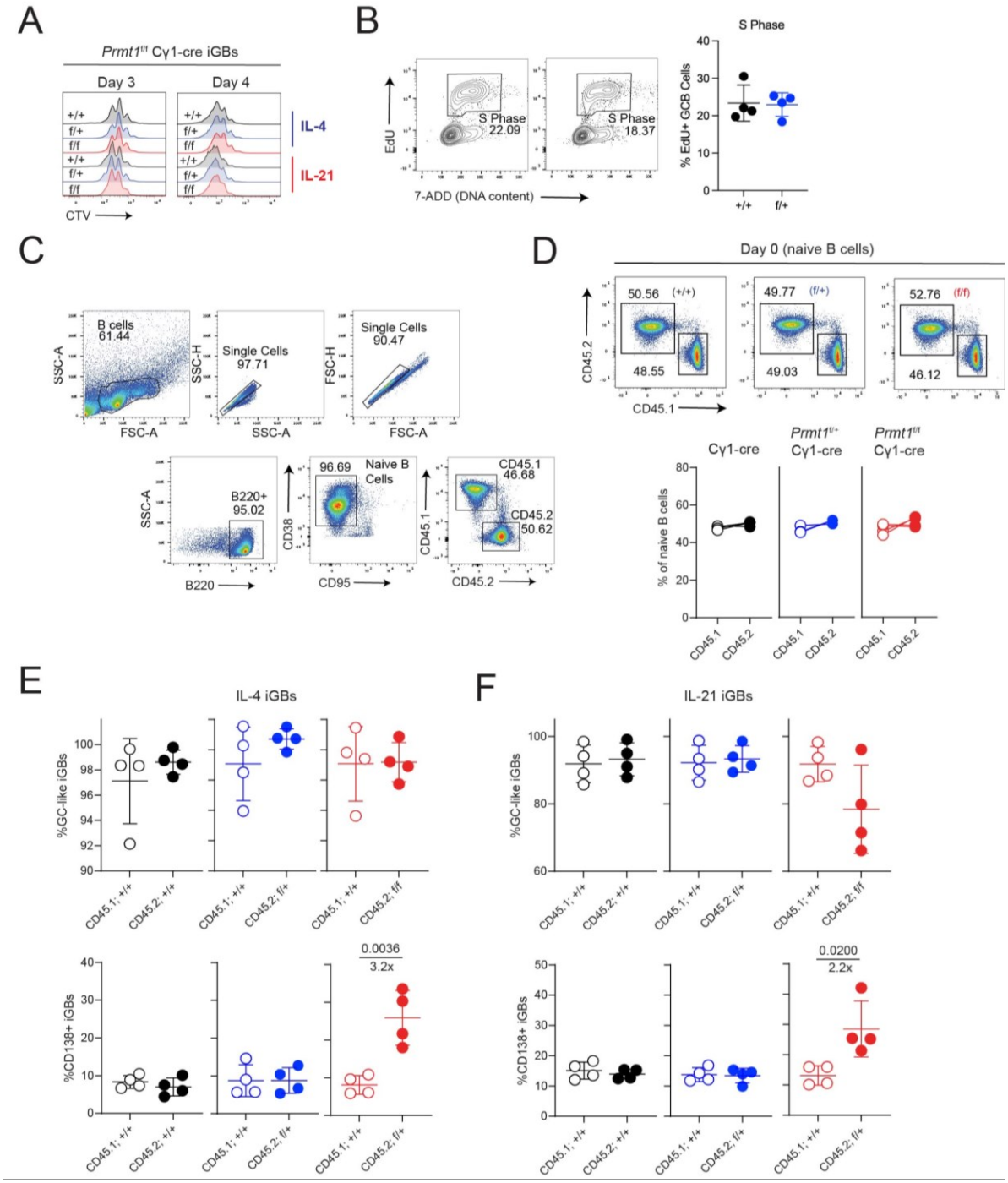

Supplementary Figure 4. *Prmt1* is haplo-sufficient for supporting normal B cell proliferation and differentiation. (A) Representative flow cytometry plots of CTV staining in Cγ1-cre, *Prmt1*$^{+/-}$ Cγ1-cre, and *Prmt1*$^{-/-}$ Cγ1-cre iGBs grown with IL-4 or IL-21. **(B)** Representative flow cytometry plots and pooled frequencies of GCB cells in S phase (EdU^{+}) from Cγ1-cre and *Prmt1*$^{+/-}$ Cγ1-cre mice 14- or 15-days post-immunization with NP-CGG. Data are representative of two independent experiments. **(C)** Gating strategy for enumerating frequencies of CD45.1^{+} and CD45.2^{+} naïve B cells (B220^{+}CD38^{+}CD95^{-}) at day 0 for iGB competitive co-cultures. **(D)** Representative flow

cytometry plots and pooled frequencies of $CD45.1^+$ and $CD45.2^+$ naïve B cells at day 0 from iGB competitive co-cultures. Data are pooled from four independent experiments. **(E)** Frequencies of $CD45.1^+$ and $CD45.2^+$ GC-like iGBs ($B220^+GL7^+CD38^-CD95^+$) from Cγ1-cre*, Prmt1*$^{+/-}$ Cγ1-cre, and *Prmt1*$^{-/-}$ Cγ1-cre competitive co-cultures. Data pooled from four independent experiments. **(F)** Frequencies of $CD45.1^+$ and $CD45.2^+$ PCs ($CD138^+$) from Cγ1-cre*, Prmt1*$^{+/-}$ Cγ1-cre, and *Prmt1*$^{-/-}$ Cγ1-cre competitive co-cultures. Data pooled from four independent experiments. P-values in (E-F) were calculated using an unpaired Student's *t*-test.

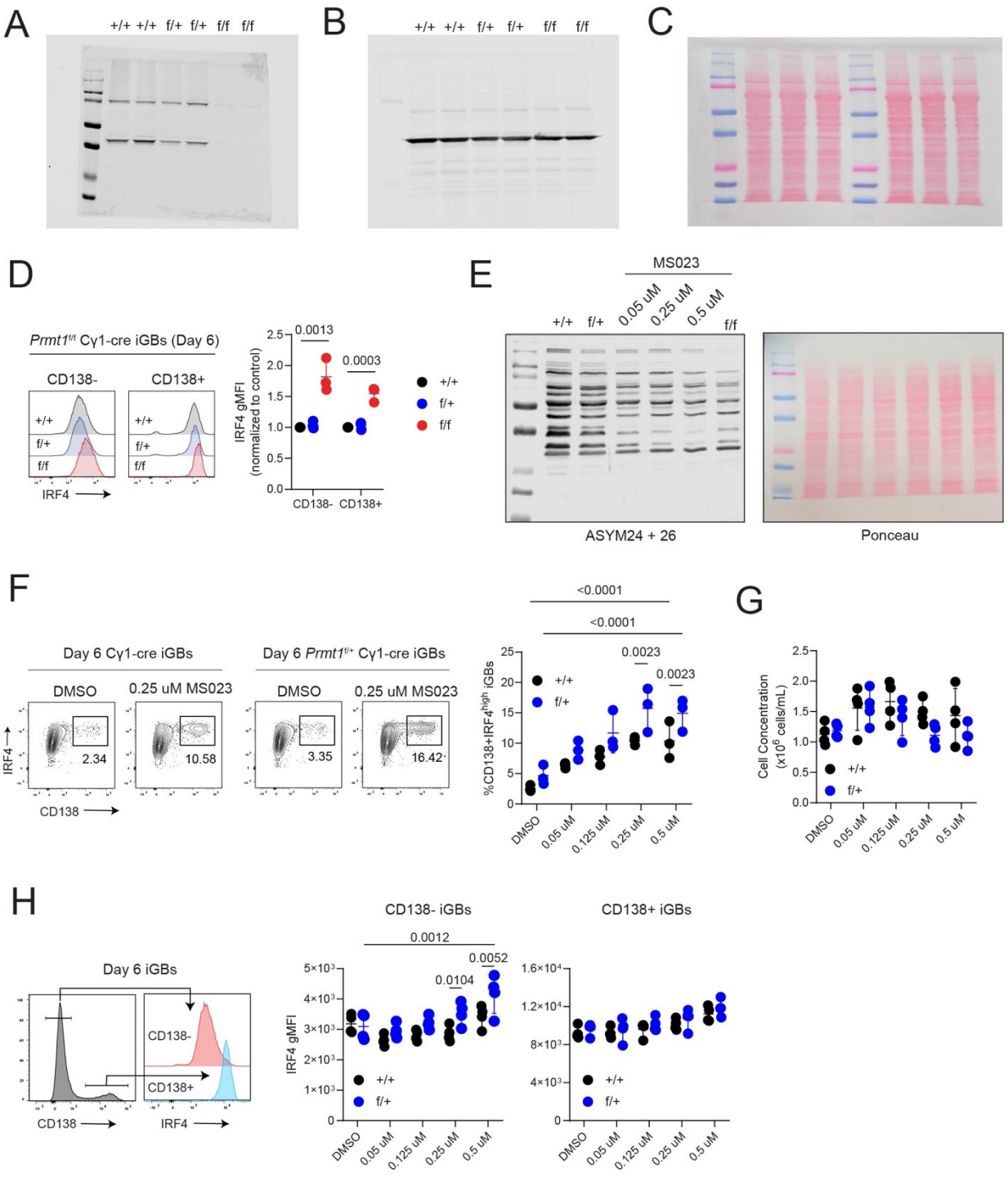

Supplementary Figure 5. *Prmt1*$^{+/-}$ Cγ1-cre iGBs are poised for PC differentiation. (A) Western blot image of PRMT1 protein expression in Cγ1-cre, *Prmt1*$^{+/-}$ Cγ1-cre, and *Prmt1*$^{-/-}$ Cγ1-cre iGBs from figure 3B. **(B)** Western blot image of asymmetrically di-methylated arginine in Cγ1-cre, *Prmt1*$^{+/-}$ Cγ1-cre, and *Prmt1*$^{-/-}$ Cγ1-cre iGBs from figure 3C. **(C)** Ponceau staining of blot from (B). **(D)** Representative flow cytometry plots and normalized protein expression levels (geometric mean fluorescence intensity, gMFI) of IRF4 between CD138^{+} and CD138^{-} Cγ1-cre, *Prmt1*$^{+/-}$ Cγ1-

cre, and *Prmt1*$^{-/-}$ Cγ1-cre iGBs. Data are pooled from three independent experiments. P-values calculated by One-Way ANOVA with Dunnett's multiple comparison test. **(E)** Western blot of asymmetrically methylated arginine substrates in Cγ1-cre iGBs treated with a Type I PRMT inhibitor (MS023) as well as in untreated Cγ1-cre, *Prmt1*$^{+/-}$ Cγ1-cre and *Prmt1*$^{-/-}$ Cγ1-cre iGBs. Ponceau staining of the same membrane was used to control for protein loading. **(F)** Representative flow cytometry plots and pooled frequencies of IRF4^{high}CD138^{+} PCs at day 6 from Cγ1-cre and *Prmt1*$^{+/-}$ Cγ1-cre iGBs treated with increasing doses of the MS023 inhibitor. Data are pooled from two independent experiments. **(G)** Cell counts of MS023-treated Cγ1-cre and *Prmt1*$^{+/-}$ Cγ1-cre iGBs. **(H)** Representative flow cytometry plots and protein expression levels of IRF4 (gMFI) between CD138^{+} and CD138^{-} Cγ1-cre and *Prmt1*$^{+/-}$ Cγ1-cre iGBs treated with MS023. Data in (G-H) are pooled from three independent experiments. P-values in (F) and (H) were calculated by Two-Way ANOVA with Tukey's multiple comparisons test.

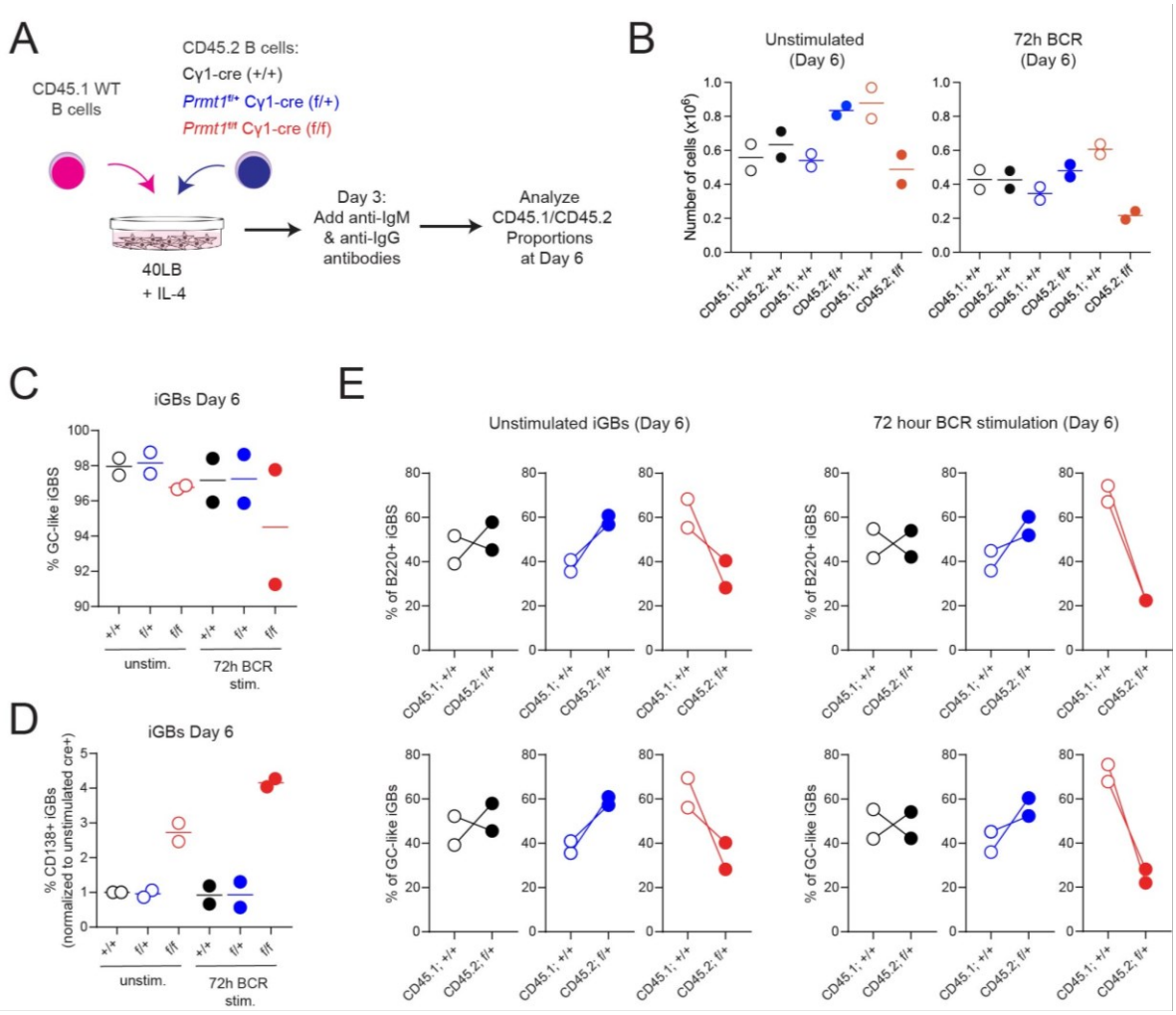

Supplementary Figure 6. *Prmt1*-deficient B cells are prone to BCR-induced growth inhibition and PC differentiation. (A) Experimental scheme for assessing the impact of BCR stimulation on iGB growth and fitness. **(B)** Cell counts of CD45.1^{+} and CD45.2^{+} iGBs at day 6 grown with or without BCR stimulation. **(C)** Pooled frequencies of CD45.1^{+} and CD45.2^{+} GC-like iGBs. **(D)**

Pooled frequencies of $CD45.1^+$ and $CD45.2^+$ PCs. **(E)** Pooled proportions of $CD45.1^+$ and $CD45.2^+$ cells among all iGBs. **(F)** Pooled proportions of $CD45.1^+$ and $CD45.2^+$ cells among all GC-like iGBs. All data are representative of two independent experiments.

Chapter IV: Discussion

PRMT1 has a well-established role in controlling B cell development as well as T-dependent and T-independent antibody responses in the periphery. PRMT1 promotes normal B cell development in the bone marrow by restricting pre-B cell proliferation (Dolezal et al., 2017). PRMT1 is also indispensable for mature B cell survival and antibody production (Hata et al., 2016; Infantino et al., 2017), and in GCB cells, PRMT1 limits the differentiation of GCB cells towards the MBC and PC fates, supporting continuous DZ-to-LZ cycling and affinity maturation (Litzler et al., 2023). Here, we reveal a dual role of *Prmt1* protein dosage in limiting both the fitness and differentiation of GCB cells and PCs, at least in part by interacting with IL-4 and IL-21 cytokine signalling. While complete *Prmt1* deficiency in activated B cells impairs GCB cell expansion and fitness, the monoallelic deletion of *Prmt1* in activated B cells increases splenic GCB cell frequencies and heightens antibody production, which we linked to heightened B cell fitness *ex vivo*. Our study highlights the importance of protein arginine methylation in controlling B cell activation and fitness.

Compared to other PTMs, protein arginine methylation is regarded as being relatively stable: arginine methylated substrates increase dramatically in activated B cells from their naïve state, and they remain stable for at least three hours post-activation (Infantino et al., 2017). However, the stoichiometry and expression of arginine-methylated proteins vary during cellular activation and differentiation, demonstrating arginine methylation can be dynamic (Geoghegan et al., 2015). In *Prmt1*$^{+/-}$ Cγ1-cre B cells, only subtle changes in arginine methylated substrates were observed. Even so, reducing PRMT1 protein dosage by half had significant consequences on B cell fitness, activation, and the GC response. Adding to previous investigations of PRMT1 in mature B cells and GCB cells (Infantino et al., 2017; Litzler et al., 2023), we identified several

bands of asymmetrically methylated proteins that were noticeably sensitive to changes in PRMT1 protein dosage. These bands most likely represent specific substrates for PRMT1 in activated B cells and could form the basis for future work to fully delineate the molecular pathways governed by *Prmt1* in GCB cells. PRMT1-mediated arginine methylation is also described to positively control the half-life of substrate proteins, such as for E2F1 and DDX3 (Hsu et al., 2024; Zheng et al., 2013), and we could speculate that the substrates with a shortest half-life would be the most sensitive to changes in PRMT1 dosage. In the future, it will be interesting to investigate how PRMT1 protein dosage controls the relative stability of substrate proteins in B cells. Such investigations will be necessary for furthering our understanding of PRMT1-mediated arginine methylation in controlling GCB cell proliferation, differentiation, and survival.

A critical finding from our study was the responsiveness of *Prmt1*$^{+/-}$ Cγ1-cre and *Prmt1*$^{-/-}$ Cγ1-cre iGBs to IL-21. IL-21 is a pleotropic cytokine produced by T_{FH} cells. Production of IL-21 increases as GC responses progress (Gonzalez et al., 2018), with critical roles in inducing PC differentiation as well as upregulating c-Myc expression and inducing PI3K/AKT/mTOR activation (Luo et al., 2023; Petersone et al., 2023; Zotos et al., 2021). The fitness advantage of *Prmt1*$^{+/-}$ Cγ1-cre iGBs was noticeably enhanced after IL-21 was added to the competitive co-cultures compared to IL-4 alone. Similarly, the growth and fitness of *Prmt1*-deficient iGBs was seemingly rescued by the addition of IL-21, and IL-21 significantly elevated *Prmt1*$^{-/-}$ Cγ1-cre PC fitness. Importantly, activation of ribosomal protein S6 — a read-out for mTOR activation — was significantly elevated in *Prmt1*$^{+/-}$ Cγ1-cre and *Prmt1*$^{-/-}$ Cγ1-cre iGBs stimulated with IL-21. Collectively, these data suggest *Prmt1* dosage fine-tunes the signals induced by IL-21R ligation in B cells. Further work will be needed to dissect the exact contribution of *Prmt1* within the IL21R/PI3K/AKT/mTOR pathway in GCB cells. S6 kinase 2 (S6K2), one of the two kinases

responsible for S6 activation, is a bona fide PRMT1 substrate in HEK293 cells (Khalil et al., 2023). PRMT1-mediated arginine methylation also blocks the phosphorylation and activation AKT substrates that are known to promote GCB cell proliferation and positive selection, notably FOXO1, whose expression is also upregulated by IL-21 in GCB cells (Inoue et al., 2017; Petersone et al., 2023; Yamagata et al., 2008). Determining whether PRMT1 methylates these substrates in activated B cells would lend insight into the regulation of IL-21 signalling by protein arginine methylation. It is also presently unclear whether other pathways downstream of IL-21 are altered in *Prmt1*$^{+/-}$ Cγ1-cre and *Prmt1*$^{-/-}$ Cγ1-cre B cells. For instance, IL-21 upregulates c-Myc, another critical mediator of GCB cell expansion. Determining whether c-Myc expression is similarly elevated in *Prmt1*$^{+/-}$ Cγ1-cre and *Prmt1*$^{-/-}$ Cγ1-cre iGBs will be important. Indeed, *Prmt1* is highly expressed in LZ GCB cells upregulating the positive selection signals, c-Myc and mTOR (Litzler et al., 2023). Furthermore, PRMT1-mediated arginine methylation is described to directly regulate c-Myc transcriptional activity in various cell types (Favia et al., 2019; Tikhanovich et al., 2017). Unravelling the interaction of PRMT1 and IL-21 signalling in GCB cells will be imperative for gaining insight into the role of arginine methylation in GC selection.

Our competitive co-culture assays also suggest a differential interaction of IL-4 and IL-21 signalling with PRMT1 protein dosage in activated B cells. Here, we find that PC fitness was significantly elevated by IL-21 compared to IL-4 in *Prmt1*$^{-/-}$ Cγ1-cre iGBs, even though IL-4 more robustly increased PC differentiation with complete *Prmt1* deficiency. Similarly, IL-21 elevated the fitness of *Prmt1*$^{+/-}$ Cγ1-cre iGBs and fully rescued the growth defect of *Prmt1*$^{-/-}$ Cγ1-cre iGBs. T_{FH}-derived IL-4 and IL-21 activate B cells through distinct JAK-STAT signalling pathways: IL-4 primarily signals through STAT6 (Haniuda et al., 2020; Turqueti-Neves et al., 2014; Wurster et al., 2002; Zhu et al., 2001), while IL-21 signals through STAT3 (Avery et al., 2010; Fike et al.,

2023; Luo et al., 2023). However, IL-4 can also activate STAT3 (Haniuda et al., 2020). PRMT1 is known to regulate STAT protein activity in immune cells and cancer cells. In T cells, PRMT1 promotes the recruitment of STAT3 to the *IL-17* locus, promoting IL-17 expression and T_H17 differentiation (Sen et al., 2018). PRMT1 also catalyzes the asymmetric di-methylation of STAT3 at Arg688 to promote osteosarcoma metastasis (Yang et al., 2022), and PRMT1 activity restricts anti-tumor immunity by negatively regulating STAT1 signalling in melanoma cells (Djajawi et al., 2024). Future work will be needed to assess the role of *Prmt1* in controlling STAT protein expression, activation, and recruitment to target genes in B cells following IL-4 and IL-21 stimulation, which could be addressed by immunoblotting and ChIP-seq. IL-4 and IL-21 production by T_{FH} cells also evolves as the GC reaction progresses: IL-21 expression begins at earlier time points, whereas IL-4 expression is detectable at later time points (Gonzalez et al., 2018; Weinstein et al., 2016). We could speculate that the arginine methylation requirements might change as B cells progress through the GC reaction and respond to T_{FH}-derived IL-4 and IL-21. Understanding how PRMT1-mediated arginine methylation interacts with IL-4 and IL-21 signalling in GCB cells *in vivo* will be necessary to expand our understanding on how PRMT1 controls GCB cell proliferation, differentiation, and fitness in response to cytokine signalling.

The opposing effects of completely versus partially deleting *Prmt1* on B cell fitness coincided with divergent consequences on the antibody response. Owing to the impaired expansion of GCs in *Prmt1*$^{-/-}$ Cγ1-cre mice immunized with NP-CGG (Litzler et al., 2023), anti-NP IgG1 production and affinity are reduced. Anti-NP IgG1 titres in *Prmt1*$^{+/-}$ Cγ1-cre mice were largely normal. However, total anti-NP IgM titers were elevated in *Prmt1*$^{+/-}$ Cγ1-cre mice, and titers of high-affinity anti-NP2 IgM antibodies — which would have been generated by affinity maturation during the GC reaction — were increased, aligning with the elevated GCB cell response in *Prmt1*$^{+/-}$

Cγ1-cre mice. In Cγ1-cre transgenic mice, IgM^+ B cells are thought to represent GCB cells that express Cγ1 germline transcripts and *Aicda* transcripts without undergoing class-switching to IgG1 (Casola et al., 2006). The differential effect of *Prmt1* heterozygosity on anti-NP IgM and IgG1 antibody production may reflect the intrinsic selective advantages of IgM and IgG1 antibodies. NP responses mature rapidly and are dominated by intra-clonal competition (Le et al., 2008). NP-CGG plus Alum also preferentially induces switching to IgG1 (Esser and Radbruch, 1990; Jack et al., 1977; Perlmutter et al., 1978). Moreover, $IgG1^+$ GCB cells are already heavily selected during the GC response and outcompete IgM^+ GCB cells as the immune response progresses (Sundling et al., 2021). Polyclonal anti-CGG IgG1 and IgG production — a response that involves both intra- and inter-clonal competition — was also significantly elevated in *Prmt1*$^{+/-}$ Cγ1-cre mice, contrasting with the drastic reduction in anti-CGG IgG1 antibodies in immunized *Prmt1*$^{-/-}$ Cγ1-cre mice. These findings align with the elevated proportion of PCs in immunized *Prmt1*$^{+/-}$ Cγ1-cre mice *in vivo* as well as the clear increase in PC fitness in *ex vivo* generated *Prmt1*$^{+/-}$ Cγ1-cre PCs. The elevated antibody response in *Prmt1*$^{+/-}$ Cγ1-cre mice was also observed in non-immunized mice, specifically by an increase in IgM antibody production, which would most likely originate from long-lived IgM^+ PCs in the bone marrow or spleen. In the future, it would be useful to understand the role of arginine methylation in controlling the long-term survival of PCs in *Prmt1*$^{+/-}$ Cγ1-cre mice such as by analyzing their persistence in the spleen or by tracking their homing to the bone marrow following an acute immunization.

Considerable attention has also been placed on the regulation of BCR signalling by *Prmt1* in pre-B cells and follicular B cells. BCR ligation in *Prmt1*-deficient B cells heightens the activity of PI3K/ERK pathways and dampens the activation of FOXO1, a transcription factor necessary for GC formation, class-switching, and affinity maturation (Dengler et al., 2008; Dominguez-Sola

et al., 2015; Infantino et al., 2010; Infantino et al., 2017; Inoue et al., 2017). Our data indirectly support the notion that BCR signalling is similarly altered when *Prmt1* is deleted following B cell activation, as evidenced by heightened plasmablast differentiation and diminished fitness in BCR-stimulated *Prmt1*$^{-/-}$ Cγ1-cre iGBs. *Prmt1*$^{+/-}$ Cγ1-cre iGBs were not responsive to BCR-induced PB differentiation, nor did BCR ligation have any noticeable effect on their growth or fitness compared to Cγ1-cre iGBs. We conclude that *Prmt1* heterozygosity does not affect BCR signalling. It is possible that the arginine residue methylated on the BCR Igα subunit has a relatively long half-life, and hence, is less sensitive to variations in PRMT1 protein dosage. It is also plausible that other PRMTs could compensate for the loss of PRMT1 protein expression in *Prmt1*$^{+/-}$ Cγ1-cre iGBs to ensure BCR signalling remains functionally intact. For instance, knockdown of *Prmt1* increases substrate scavenging by other PRMTs, notably PRMT5, an arginine methyltransferase that is also suggested to control BCR signalling in B cell lymphoma (Sloan et al., 2023; Zhu et al., 2019). The extent to which alternative PRMT-mediated methylation patterns are affected in *Prmt1*$^{+/-}$ Cγ1-cre iGBs — and how they might even contribute to the fitness advantage of *Prmt1*$^{+/-}$ Cγ1-cre B cells — will need to be explored. Such investigations would also inform strategies for targeting PRMT1 and other PRMTs in B cell lymphoma.

Studies investigating PRMT1 in the context of lymphoma have largely focused on the therapeutic potential of downregulating PRMT1 activity. PRMT1 is overexpressed in patients with DLBCL and is associated with poor clinical outcomes (Leonard et al., 2012; Litzler et al., 2023). Type I PRMT inhibitors also block the growth of B cell lymphoma cell lines *in vitro* and in xenograft mouse models (Fedoriw et al., 2019). However, a recent clinical trial investigating the therapeutic potential of the Type I PRMT inhibitor, GSK3368715, in patients with DLBCL reported a poor therapeutic efficacy (El-Khoueiry et al., 2023). The poor efficacy of GSK3368715

could have arisen from the interplay between Type I and Type II PRMTs in cancer cells (El-Khoueiry et al., 2023; Fedoriw et al., 2019; Gao et al., 2019; Nguyen et al., 2023). Heterogeneity in the patient population may have also contributed to the study's findings (El-Khoueiry et al., 2023). Here, we indicate that the reduction of PRMT1 protein expression by half in activated B cells has the potential to augment B cell fitness. Our findings provide additional explanations for the poor efficacy of Type I PRMT inhibitors in patients with B cell lymphoma and warrant further investigations into how PRMT1 protein dosage may contribute to the fitness of B cell lymphomas.

There has also been little attention on whether disruptions in PRMT1 activity promote lymphomagenesis, as is the case for leukemia. Bona fide co-activators of PRMT1, notably BTG1 and BTG2, are commonly mutated in DLBCL (De Simone et al., 2023; Delage et al., 2023). BTG1 and BTG2 belong to the BTG/TOB protein family and generally act as tumor suppressors (Schmitz et al., 2018; Zhang et al., 2023), although BTG1 does have oncogenic roles in GC-derived lymphomas. In mice, *BTG1* missense mutations elevate the fitness of GC-derived B cell lymphoma through enhanced c-Myc protein synthesis and mTOR signalling, accelerating lymphomagenesis (Mlynarczyk et al., 2023). BTG2 super-enhancer mutations that downregulate BTG2 expression have also been linked to the development of lymphoma (De Simone et al., 2023). BTG1 and BTG2 are well-described co-activators of PRMT1 (Berthet et al., 2002), and perturbations in BTG1 or BTG2 can directly affect PRMT1 substrate binding and methylation. BTG2 knockdown reduces PRMT1-mediated arginine methylation in B cell precursors and leukemia, elevating the growth of leukemia cells *in vivo* (Dolezal et al., 2017). Indeed, the overexpression of BTG2 in pre-B cells promotes differentiation, which is dependent on PRMT1. In mouse embryonic fibroblasts and bone marrow-derived B cell progenitors, loss of *Btg1* confers a cell-intrinsic survival advantage following cellular stress responses. Mechanistically, *Btg1* loss abrogates PRMT1-mediated

methylation and activation of the cellular stress response protein, Activating Transcription Factor 4 (ATF4), which otherwise promotes cell death under cellular stress conditions (Yuniati et al., 2016). *Btg1* knock-down in pre-B acute lymphoblastic leukemia (ALL) also confers resistance to glucocorticoid therapies, which depends on the regulation of glucocorticoid receptor expression by PRMT1, although *PRMT1* knockdown does not recapitulate the phenotype of *BTG1* deficiency in pre-B ALL cells (van Galen et al., 2010). Collectively, these data suggest that selective or total disruptions in PRMT1-mediated arginine methylation have the potential to elevate cellular fitness, either directly through *PRMT1* depletion or indirectly through the depletion of bona fide PRMT1 co-activators. BTG1 and BTG2 are commonly mutated in activated B cell (ABC)-DLBCL, which are lymphomas derived from plasmablasts (Schmitz et al., 2018). But whether *BTG1* or *BTG2* mutations affect PRMT1 activity in ABC-DLBCL is unknown. PRMT1 is preferentially expressed in DLBCL samples upregulating c-Myc and mTOR, especially among lymphoma samples exhibiting a GCB cell-like phenotype (Goverdhan et al., 2017; Litzler et al., 2023; Xu-Monette et al., 2016). PRMT1 inhibition also potently inhibits the growth of GCB-like DLBCL cell lines more efficiently than ABC-like DLBCL cell lines (Goverdhan, 2017). In the future, it will be necessary to determine the frequency of PRMT1 mutations across different DLBCL subtypes and whether there are alterations in the PRMT1 activity following *BTG1* or *BTG2* loss in human B cell lymphoma. It would also be informative to understand the differential dependency of DLCBL subtypes on PRMT1 activity. Such work would further elucidate the therapeutic potential of targeting PRMT1 in B cell lymphoma.

Conclusion

In the present work, we outline the role of PRMT1 protein dosage in restricting the fitness and differentiation of GCB cells and PCs. The monoallelic deletion of *Prmt1* in activated B cells resulted in elevated frequencies of splenic GCB cells and PCs in response to an acute immunization, in addition to increasing IgM and IgG antibody production without visibly affecting affinity maturation. Aligning with the enhanced antibody response in *Prmt1*$^{+/-}$ Cγ1-cre mice, the partial deficiency of *Prmt1* in activated B cells imparted a fitness advantage to *ex vivo*-generated GCB cells and PCs in the presence of IL-4, which was augmented by IL-21 and associated with elevated mTOR activation. Furthermore, we provide evidence for the differential interaction of IL-4 and IL-21 cytokine signalling by *Prmt1* in activated B cells. We conclude that *Prmt1* protein dosage is a critical determinant of GCB cell and PC fitness, directly interacting with cytokine signalling pathways involved in positive selection and GCB cell differentiation. This work expands our understanding on how arginine methylation controls humoral immunity. Further work will be necessary to dissect the mechanism through which PRMT1 intersects with IL-4 and IL-21 signalling in GCB cells, in addition to investigating potential role of *Prmt1* heterozygosity in lymphomagenesis. Importantly, this work provides potential explanations for the poor efficacy of Type I PRMT inhibitors in patients with B cell lymphoma.

Supplementary Tables

Table S1: Antibodies used for flow cytometry and ELISAs.

Antibody	Manufacturer	Catalogue Number	Dilution or Concentration
Rat Anti-Mouse/Human CD45R/B220 Alexa Fluor 700 (clone: RA3-6B2)	BioLegend	103232	1/200
Rat Anti-Mouse IgD FITC (clone: 11-26c.2$\boldsymbol{\alpha}$)	BD Pharmingen	553439	1/200
Rat Anti-Mouse/Human GL7 Pacific Blue (clone: GL7)	BioLegend	144614	1/200
Rat Anti-Mouse GL7 Alexa Fluor 647 (clone: GL7)	BD Pharmingen	561529	1/200
Hamster Anti-Mouse CD95/Fas Alexa Fluor 647 (clone: Jo2)	BD Pharmingen	563647	1/200
Hamster Anti-Mouse CD95/Fas PE-Cy7 (clone: Jo2)	BD Pharmingen	557653	1/200
Hamster Anti-Mouse CD95/Fas FITC (clone: Jo2)	BD Pharmingen	554257	1/200
Rat Anti-Mouse B7-2/CD86 Biotin (clone: GL1)	Invitrogen	13-0862-82	1/100
Rat Anti-Mouse CXCR4/CD184 PE (clone: 2B11)	Invitrogen	12-9991-82	1/100
Rat Anti-Mouse CXCR4/CD184 PerCP-eFluor 710 (clone: 2B11)	Invitrogen	46-9991-80	1/100
Hamster Anti-Mouse CCR6 PE-Cy7 (clone: 29-2L17)	BioLegend	129816	1/100
Rat Anti-Mouse IgM BV421 (clone: R6-60.2)	BD Pharmingen	562595	1/50
Rat Anti-Mouse IgG1 PE (clone: A85-1)	BD Pharmingen	550083	1/500
Rat Anti-Mouse CD138 BV605 (clone: 281-2)	BD Pharmingen	563147	1/100
Rat Anti-Mouse CD4 FITC (clone: RM4-5)	Invitrogen	11-0042-82	1/200
Rat Anti-Mouse/Human CD44 PE-Cy7 (clone: IM7)	Invitrogen	25-0441-81	1/300
Rat Anti-Mouse CD62L/L-Selectin APC (clone: MEL-14)	Invitrogen	17-0621-81	1/200
Rat Anti-Bovine/Dog/Cat/Mouse/Pig/Rat FOXP3 PE (clone: FJK-16s)	Invitrogen	12-5773-80	1/200
Mouse Anti-Mouse BCL6 BV421 (clone: K112-91)	BD Pharmingen	563363	1/20
Hamster Anti-Mouse PD-1 PerCP-eFluor 710 (clone: J43)	Invitrogen	46-9985-80	1/100
Rat Anti-Mouse CXCR5/CD185 Biotin (clone: SPRCL5)	Invitrogen	13-7185-82	1/25

Rat Anti-Mouse CD38 PE (clone: 90)	BioLegend	102708	1/200
Mouse Anti-Mouse/Human RPS6 Phospho (Ser235/Ser236) PE (clone: A17020B)	BioLegend	608603	1/200
Rat Anti-Mouse/Human IRF4 PE (clone: 3E4)	Invitrogen	12-9858-82	1/50
Mouse Anti-Mouse CD45.1 APC (clone: A20)	BD Pharmingen	558701	1/200
Mouse Anti-Mouse CD45.2 APC-Cy7 (clone: 104)	BD Pharmingen	560694	1/200
Streptavidin BV605	BioLegend	405229	1/100
Mouse Biotin APC	Miltenyi Biotec	Bio3-18E7	1/200
Mouse IgM, κ Isotype Control (clone: G155-228)	BD Pharmingen	553472	–
Rat Anti-Mouse IgM (clone: II/41)	BD Pharmingen	553435	2 ug/mL
Biotin Rat Anti-Mouse IgM (clone: R6-60.2)	BD Pharmingen	553406	1/500
Mouse IgG1, κ Isotype Control (clone: MOPC-31C)	BD Pharmingen	557273	–
Rat Anti-Mouse IgG1 (clone: A85-3)	BD Pharmingen	553445	2 ug/mL
Biotin Rat Anti-Mouse IgG1 (clone: A85-1)	BD Pharmingen	553441	1/1000
Mouse IgG2b, κ Isotype Control (clone: MPC-11)	BD Pharmingen	557351	–
Rat Anti-Mouse IgG2b (clone: R9-91)	BD Pharmingen	553396	2 ug/mL
Biotin Rat Anti-Mouse IgG2b (clone: R12-3)	BD Pharmingen	553393	1/1000
Mouse IgG3, κ Isotype Control (clone: A112-3)	BD Pharmingen	553486	–
Rat Anti-Mouse IgG3 (clone: R2-38)	BD Pharmingen	553404	2 ug/mL
Biotin Rat Anti-Mouse IgG3 (clone: R40-82)	BD Pharmingen	553401	1/2000
Goat Anti-Mouse IgG HRP	Jackson ImmunoResearch	115-035-071	1/1000
HRP-Conjugated Streptavidin	ThermoScientific	N100	1/5000

Table S2: Antibodies used for Western blotting.

Antibody	**Manufacturer**	**Catalogue Number**	**Dilution or Concentration**
Rat anti-Human, Mouse, Rat PRMT1 (clone: 7D2)	MilliporeSigma	MABE431	1/1000
Rabbit Anti-dimethyl-Arginine Antibody, asymmetric (ASYM24)	Sigma-Aldrich	07-414	1/1000
Rabbit Asymmetric Dimethyl-arginine Antibody (ADMA) Asym26	EpiCypher	13-0011	1/1000
Rabbit Anti-Actin	Sigma-Aldrich	A2066	1/3000
Goat Anti-rabbit IgG IRDye 800CW	LICORbio	926-32211	1/20000
Goat anti-Rat IgG (H+L) Alexa Fluor 680	Invitrogen	A-21096	1/20000

References

Aghamohammadi, A., T. Cheraghi, M. Gharagozlou, M. Movahedi, N. Rezaei, M. Yeganeh, N. Parvaneh, H. Abolhassani, Z. Pourpak, and M. Moin. 2009. IgA deficiency: correlation between clinical and immunological phenotypes. *J Clin Immunol*. 29:130-136.

Allen, C.D.C., K.M. Ansel, C. Low, R. Lesley, H. Tamamura, N. Fujii, and J.G. Cyster. 2004. Germinal center dark and light zone organization is mediated by CXCR4 and CXCR5. *Nature Immunology*. 5:943-952.

Allen, D., T. Simon, F. Sablitzky, K. Rajewsky, and A. Cumano. 1988. Antibody engineering for the analysis of affinity maturation of an anti-hapten response. *Embo j*. 7:1995-2001.

Amzel, L.M., and R.J. Poljak. 1979. Three-dimensional structure of immunoglobulins. *Annu Rev Biochem*. 48:961-997.

Avery, D.T., E.K. Deenick, C.S. Ma, S. Suryani, N. Simpson, G.Y. Chew, T.D. Chan, U. Palendira, J. Bustamante, S. Boisson-Dupuis, S. Choo, K.E. Bleasel, J. Peake, C. King, M.A. French, D. Engelhard, S. Al-Hajjar, S. Al-Muhsen, K. Magdorf, J. Roesler, P.D. Arkwright, P. Hissaria, D.S. Riminton, M. Wong, R. Brink, D.A. Fulcher, J.-L. Casanova, M.C. Cook, and S.G. Tangye. 2010. B cell–intrinsic signaling through IL-21 receptor and STAT3 is required for establishing long-lived antibody responses in humans. *Journal of Experimental Medicine*. 207:155-171.

Bassing, C.H., W. Swat, and F.W. Alt. 2002. The mechanism and regulation of chromosomal V(D)J recombination. *Cell*. 109 Suppl:S45-55.

Bedford, M.T., and S.G. Clarke. 2009. Protein Arginine Methylation in Mammals: Who, What, and Why. *Molecular Cell*. 33:1-13.

Béguelin, W., R. Popovic, M. Teater, Y. Jiang, K.L. Bunting, M. Rosen, H. Shen, S.N. Yang, L. Wang, T. Ezponda, E. Martinez-Garcia, H. Zhang, Y. Zheng, S.K. Verma, M.T. McCabe, H.M. Ott, G.S. Van Aller, R.G. Kruger, Y. Liu, C.F. McHugh, D.W. Scott, Y.R. Chung, N. Kelleher, R. Shaknovich, C.L. Creasy, R.D. Gascoyne, K.K. Wong, L. Cerchietti, R.L. Levine, O. Abdel-Wahab, J.D. Licht, O. Elemento, and A.M. Melnick. 2013. EZH2 is required for germinal center formation and somatic EZH2 mutations promote lymphoid transformation. *Cancer Cell*. 23:677-692.

Béguelin, W., M.A. Rivas, M.T. Calvo Fernández, M. Teater, A. Purwada, D. Redmond, H. Shen, M.F. Challman, O. Elemento, A. Singh, and A.M. Melnick. 2017. EZH2 enables germinal centre formation through epigenetic silencing of CDKN1A and an Rb-E2F1 feedback loop. *Nature Communications*. 8:877.

Béguelin, W., M. Teater, C. Meydan, K.B. Hoehn, J.M. Phillip, A.A. Soshnev, L. Venturutti, M.A. Rivas, M.T. Calvo-Fernández, J. Gutierrez, J.M. Camarillo, K. Takata, K. Tarte, N.L. Kelleher, C. Steidl, C.E. Mason, O. Elemento, C.D. Allis, S.H. Kleinstein, and A.M. Melnick. 2020. Mutant EZH2 Induces a Pre-malignant Lymphoma Niche by Reprogramming the Immune Response. *Cancer Cell*. 37:655-673.e611.

Berek, C., A. Berger, and M. Apel. 1991. Maturation of the immune response in germinal centers. *Cell*. 67:1121-1129.

Berek, C., and C. Milstein. 1987. Mutation drift and repertoire shift in the maturation of the immune response. *Immunol Rev*. 96:23-41.

Berthet, C., F. Guéhenneux, V. Revol, C. Samarut, A. Lukaszewicz, C. Dehay, C. Dumontet, J.P. Magaud, and J.P. Rouault. 2002. Interaction of PRMT1 with BTG/TOB proteins in cell signalling: molecular analysis and functional aspects. *Genes Cells*. 7:29-39.

Blanc, R.S., and S. Richard. 2017. Arginine Methylation: The Coming of Age. *Molecular Cell*. 65:8-24.
Brandtzaeg, P. 2007. Induction of secretory immunity and memory at mucosal surfaces. *Vaccine*. 25:5467-5484.
Brandtzaeg, P. 2009. Mucosal Immunity: Induction, Dissemination, and Effector Functions. *Scandinavian Journal of Immunology*. 70:505-515.
Calado, D.P., Y. Sasaki, S.A. Godinho, A. Pellerin, K. Köchert, B.P. Sleckman, I.M. de Alborán, M. Janz, S. Rodig, and K. Rajewsky. 2012. The cell-cycle regulator c-Myc is essential for the formation and maintenance of germinal centers. *Nat Immunol*. 13:1092-1100.
Casadevall, A. 1998. Antibody-mediated protection against intracellular pathogens. *Trends in Microbiology*. 6:102-107.
Casola, S., G. Cattoretti, N. Uyttersprot, S.B. Koralov, J. Seagal, Z. Hao, A. Waisman, A. Egert, D. Ghitza, and K. Rajewsky. 2006. Tracking germinal center B cells expressing germ-line immunoglobulin gamma1 transcripts by conditional gene targeting. *Proc Natl Acad Sci U S A*. 103:7396-7401.
Chaudhuri, J., and F.W. Alt. 2004. Class-switch recombination: interplay of transcription, DNA deamination and DNA repair. *Nature Reviews Immunology*. 4:541-552.
Chen, H., Y. Zhang, A.Y. Ye, Z. Du, M. Xu, C.-S. Lee, J.K. Hwang, N. Kyritsis, Z. Ba, D. Neuberg, D.R. Littman, and F.W. Alt. 2020. BCR selection and affinity maturation in Peyer's patch germinal centres. *Nature*. 582:421-425.
Chen, S.T., T.Y. Oliveira, A. Gazumyan, M. Cipolla, and M.C. Nussenzweig. 2023. B cell receptor signaling in germinal centers prolongs survival and primes B cells for selection. *Immunity*. 56:547-561.e547.
Chevrier, S., T. Kratina, D. Emslie, D.M. Tarlinton, and L.M. Corcoran. 2017. IL4 and IL21 cooperate to induce the high Bcl6 protein level required for germinal center formation. *Immunol Cell Biol*. 95:925-932.
Chou, C., D.J. Verbaro, E. Tonc, M. Holmgren, M. Cella, M. Colonna, D. Bhattacharya, and T. Egawa. 2016. The Transcription Factor AP4 Mediates Resolution of Chronic Viral Infection through Amplification of Germinal Center B Cell Responses. *Immunity*. 45:570-582.
Cooper, N.R. 1985. The Classical Complement Pathway: Activation and Regulation of the First Complement Component11Publication number 3541 IMM. *In* Advances in Immunology. Vol. 37. F.J. Dixon, editor. Academic Press. 151-216.
Cyster, J.G., and C.D.C. Allen. 2019. B Cell Responses: Cell Interaction Dynamics and Decisions. *Cell*. 177:524-540.
Czajkowsky, D.M., and Z. Shao. 2009. The human IgM pentamer is a mushroom-shaped molecule with a flexural bias. *Proc Natl Acad Sci U S A*. 106:14960-14965.
De Simone, P., E. Bal, A. Holmes, L. Hilton, K. Basso, R.K. Soni, R. Morin, R. Dalla-Favera, and L. Pasqualucci. 2023. BTG2 Super-Enhancer Mutations Disrupt TFAP4 Binding and Deregulate BTG2 Expression in Diffuse Large B-Cell Lymphoma. *Blood*. 142:523.
Deisenhammer, F., G. Keir, B. Pfausler, and E.J. Thompson. 1996. Affinity of anti-GM1 antibodies in Guillain-Barré syndrome patients. *J Neuroimmunol*. 66:85-93.
Delage, L., M. Lambert, É. Bardel, C. Kundlacz, D. Chartoire, A. Conchon, A.-L. Peugnet, L. Gorka, P. Auberger, A. Jacquel, C. Soussain, O. Destaing, H.-J. Delecluse, S. Delecluse, S. Merabet, A. Traverse-Glehen, G. Salles, E. Bachy, M. Billaud, H. Ghesquières, L. Genestier, J.-P. Rouault, and P. Sujobert. 2023. BTG1 inactivation drives

lymphomagenesis and promotes lymphoma dissemination through activation of BCAR1. *Blood*. 141:1209-1220.

Deng, Q., P. Lakra, P. Gou, H. Yang, C. Meydan, M. Teater, C. Chin, W. Zhang, T. Dinh, U. Hussein, X. Li, E. Rojas, W. Liu, P.K. Reville, A. Kizhakeyil, D. Barisic, S. Parsons, A. Wilson, J. Henderson, B. Scull, C. Gurumurthy, F. Vega, A. Chadburn, B. Cuglievan, N.K. El-Mallawany, C. Allen, C. Mason, A. Melnick, and M.R. Green. 2024. SMARCA4 is a haploinsufficient B cell lymphoma tumor suppressor that fine-tunes centrocyte cell fate decisions. *Cancer Cell*. 42:605-622.e611.

Dengler, H.S., G.V. Baracho, S.A. Omori, S. Bruckner, K.C. Arden, D.H. Castrillon, R.A. DePinho, and R.C. Rickert. 2008. Distinct functions for the transcription factor Foxo1 at various stages of B cell differentiation. *Nat Immunol*. 9:1388-1398.

Dhar, S., V. Vemulapalli, A.N. Patananan, G.L. Huang, A. Di Lorenzo, S. Richard, M.J. Comb, A. Guo, S.G. Clarke, and M.T. Bedford. 2013. Loss of the major Type I arginine methyltransferase PRMT1 causes substrate scavenging by other PRMTs. *Sci Rep*. 3:1311.

Di Noia, J.M., and M.S. Neuberger. 2007. Molecular Mechanisms of Antibody Somatic Hypermutation. *Annual Review of Biochemistry*. 76:1-22.

Djajawi, T.M., L. Pijpers, A. Srivaths, D. Chisanga, K.F. Chan, S.J. Hogg, L. Neil, S.M. Rivera, N. Bartonicek, S.L. Ellis, T.C.C. Lim Kam Sian, P. Faridi, Y. Liao, B. Pal, A. Behren, W. Shi, S.J. Vervoort, R.W. Johnstone, and C.J. Kearney. 2024. PRMT1 acts as a suppressor of MHC-I and anti-tumor immunity. *Cell Rep*. 43:113831.

Dolezal, E., S. Infantino, F. Drepper, T. Börsig, A. Singh, T. Wossning, G.J. Fiala, S. Minguet, B. Warscheid, D.M. Tarlinton, H. Jumaa, D. Medgyesi, and M. Reth. 2017. The BTG2-PRMT1 module limits pre-B cell expansion by regulating the CDK4-Cyclin-D3 complex. *Nature Immunology*. 18:911-920.

Dominguez-Sola, D., J. Kung, A.B. Holmes, V.A. Wells, T. Mo, K. Basso, and R. Dalla-Favera. 2015. The FOXO1 Transcription Factor Instructs the Germinal Center Dark Zone Program. *Immunity*. 43:1064-1074.

Dominguez-Sola, D., G.D. Victora, C.Y. Ying, R.T. Phan, M. Saito, M.C. Nussenzweig, and R. Dalla-Favera. 2012. The proto-oncogene MYC is required for selection in the germinal center and cyclic reentry. *Nat Immunol*. 13:1083-1091.

Dong, Y., R. Tu, H. Liu, and G. Qing. 2020. Regulation of cancer cell metabolism: oncogenic MYC in the driver's seat. *Signal Transduction and Targeted Therapy*. 5:124.

Draghi, N.A., and L.K. Denzin. 2010. H2-O, a MHC class II-like protein, sets a threshold for B-cell entry into germinal centers. *Proceedings of the National Academy of Sciences*. 107:16607-16612.

Duan, L., D. Liu, H. Chen, M.A. Mintz, M.Y. Chou, D.I. Kotov, Y. Xu, J. An, B.J. Laidlaw, and J.G. Cyster. 2021. Follicular dendritic cells restrict interleukin-4 availability in germinal centers and foster memory B cell generation. *Immunity*. 54:2256-2272.e2256.

Dvorscek, A.R., C.I. McKenzie, M.J. Robinson, Z. Ding, C. Pitt, K. O'Donnell, D. Zotos, R. Brink, D.M. Tarlinton, and I. Quast. 2022. IL‐21 has a critical role in establishing germinal centers by amplifying early B cell proliferation. *EMBO reports*. 23:e54677.

Edelman, G.M., B.A. Cunningham, W.E. Gall, P.D. Gottlieb, U. Rutishauser, and M.J. Waxdal. 1969. THE COVALENT STRUCTURE OF AN ENTIRE γG IMMUNOGLOBULIN MOLECULE[*]. *Proceedings of the National Academy of Sciences*. 63:78-85.

Eisen, H.N. 2014. Affinity enhancement of antibodies: how low-affinity antibodies produced early in immune responses are followed by high-affinity antibodies later and in memory B-cell responses. *Cancer Immunol Res*. 2:381-392.

Eisen, H.N., and G.W. Siskind. 1964. VARIATIONS IN AFFINITIES OF ANTIBODIES DURING THE IMMUNE RESPONSE. *Biochemistry*. 3:996-1008.

El-Khoueiry, A.B., J. Clarke, T. Neff, T. Crossman, N. Ratia, C. Rathi, P. Noto, A. Tarkar, I. Garrido-Laguna, E. Calvo, J. Rodón, B. Tran, P.J. O'Dwyer, A. Cuker, and A.R. Abdul Razak. 2023. Phase 1 study of GSK3368715, a type I PRMT inhibitor, in patients with advanced solid tumors. *British Journal of Cancer*. 129:309-317.

ElTanbouly, M.A., V. Ramos, A.J. MacLean, S.T. Chen, M. Loewe, S. Steinbach, T. Ben Tanfous, B. Johnson, M. Cipolla, A. Gazumyan, T.Y. Oliveira, and M.C. Nussenzweig. 2024. Role of affinity in plasma cell development in the germinal center light zone. *J Exp Med*. 221.

Enterina, J.R., S. Sarkar, L. Streith, J. Jung, B.M. Arlian, S.J. Meyer, H. Takematsu, C. Xiao, T.A. Baldwin, L. Nitschke, M.J. Shlomchick, J.C. Paulson, and M.S. Macauley. 2022. Coordinated changes in glycosylation regulate the germinal center through CD22. *Cell Rep*. 38:110512.

Ersching, J., A. Efeyan, L. Mesin, J.T. Jacobsen, G. Pasqual, B.C. Grabiner, D. Dominguez-Sola, D.M. Sabatini, and G.D. Victora. 2017. Germinal Center Selection and Affinity Maturation Require Dynamic Regulation of mTORC1 Kinase. *Immunity*. 46:1045-1058.e1046.

Esser, C., and A. Radbruch. 1990. Immunoglobulin class switching: molecular and cellular analysis. *Annu Rev Immunol*. 8:717-735.

Favia, A., L. Salvatori, S. Nanni, L.K. Iwamoto-Stohl, S. Valente, A. Mai, F. Scagnoli, R.A. Fontanella, P. Totta, S. Nasi, and B. Illi. 2019. The Protein Arginine Methyltransferases 1 and 5 affect Myc properties in glioblastoma stem cells. *Scientific Reports*. 9:15925.

Fedoriw, A., S.R. Rajapurkar, S. O'Brien, S.V. Gerhart, L.H. Mitchell, N.D. Adams, N. Rioux, T. Lingaraj, S.A. Ribich, M.B. Pappalardi, N. Shah, J. Laraio, Y. Liu, M. Butticello, C.L. Carpenter, C. Creasy, S. Korenchuk, M.T. McCabe, C.F. McHugh, R. Nagarajan, C. Wagner, F. Zappacosta, R. Annan, N.O. Concha, R.A. Thomas, T.K. Hart, J.J. Smith, R.A. Copeland, M.P. Moyer, J. Campbell, K. Stickland, J. Mills, S. Jacques-O'Hagan, C. Allain, D. Johnston, A. Raimondi, M. Porter Scott, N. Waters, K. Swinger, A. Boriack-Sjodin, T. Riera, G. Shapiro, R. Chesworth, R.K. Prinjha, R.G. Kruger, O. Barbash, and H.P. Mohammad. 2019. Anti-tumor Activity of the Type I PRMT Inhibitor, GSK3368715, Synergizes with PRMT5 Inhibition through MTAP Loss. *Cancer Cell*. 36:100-114.e125.

Feng, Y., R. Maity, J.P. Whitelegge, A. Hadjikyriacou, Z. Li, C. Zurita-Lopez, Q. Al-Hadid, A.T. Clark, M.T. Bedford, J.Y. Masson, and S.G. Clarke. 2013. Mammalian protein arginine methyltransferase 7 (PRMT7) specifically targets RXR sites in lysine- and arginine-rich regions. *J Biol Chem*. 288:37010-37025.

Fike, A.J., S.B. Chodisetti, N.E. Wright, K.N. Bricker, P.P. Domeier, M. Maienschein-Cline, A.M. Rosenfeld, S.A. Luckenbill, J.L. Weber, N.M. Choi, E.T. Luning Prak, M. Mandal, M.R. Clark, and Z.S.M. Rahman. 2023. STAT3 signaling in B cells controls germinal center zone organization and recycling. *Cell Reports*. 42:112512.

Finkin, S., H. Hartweger, T.Y. Oliveira, E.E. Kara, and M.C. Nussenzweig. 2019. Protein Amounts of the MYC Transcription Factor Determine Germinal Center B Cell Division Capacity. *Immunity*. 51:324-336.e325.

Fleischman, J.B., R.R. Porter, and E.M. Press. 1963. THE ARRANGEMENT OF THE PEPTIDE CHAINS IN GAMMA-GLOBULIN. *Biochem J*. 88:220-228.
Gao, G., L. Zhang, O.D. Villarreal, W. He, D. Su, E. Bedford, P. Moh, J. Shen, X. Shi, M.T. Bedford, and H. Xu. 2019. PRMT1 loss sensitizes cells to PRMT5 inhibition. *Nucleic Acids Res*. 47:5038-5048.
Geisberger, R., M. Lamers, and G. Achatz. 2006. The riddle of the dual expression of IgM and IgD. *Immunology*. 118:429-437.
Geoghegan, V., A. Guo, D. Trudgian, B. Thomas, and O. Acuto. 2015. Comprehensive identification of arginine methylation in primary T cells reveals regulatory roles in cell signalling. *Nature Communications*. 6:6758.
Gitlin, A.D., Z. Shulman, and M.C. Nussenzweig. 2014. Clonal selection in the germinal centre by regulated proliferation and hypermutation. *Nature*. 509:637-640.
Glaviano, A., A.S.C. Foo, H.Y. Lam, K.C.H. Yap, W. Jacot, R.H. Jones, H. Eng, M.G. Nair, P. Makvandi, B. Geoerger, M.H. Kulke, R.D. Baird, J.S. Prabhu, D. Carbone, C. Pecoraro, D.B.L. Teh, G. Sethi, V. Cavalieri, K.H. Lin, N.R. Javidi-Sharifi, E. Toska, M.S. Davids, J.R. Brown, P. Diana, J. Stebbing, D.A. Fruman, and A.P. Kumar. 2023. PI3K/AKT/mTOR signaling transduction pathway and targeted therapies in cancer. *Molecular Cancer*. 22:138.
Gonzalez, D.G., C.M. Cote, J.R. Patel, C.B. Smith, Y. Zhang, K.M. Nickerson, T. Zhang, S.M. Kerfoot, and A.M. Haberman. 2018. Nonredundant Roles of IL-21 and IL-4 in the Phased Initiation of Germinal Center B Cells and Subsequent Self-Renewal Transitions. *J Immunol*. 201:3569-3579.
Gould, H.J., and B.J. Sutton. 2008. IgE in allergy and asthma today. *Nature Reviews Immunology*. 8:205-217.
Goverdhan, A. 2017. Targeting Epigenetic Regulators For The Treatment Of Diffuse Large B-Cell Lymphoma. *In* Graduate School of Biomedical Sciences. Vol. Doctor of Philosophy. The University of Texas Dissertations and Theses (Open Access).
Goverdhan, A., H.-H. Lee, O. Havranek, R.E. Davis, and M.-C. Hung. 2017. Abstract 13: PRMT1 as a therapeutic target in diffuse large B-cell lymphoma. *Clinical Cancer Research*. 23:13-13.
Haniuda, K., S. Fukao, and D. Kitamura. 2020. Metabolic Reprogramming Induces Germinal Center B Cell Differentiation through Bcl6 Locus Remodeling. *Cell Reports*. 33:108333.
Hannum, L.G., A.M. Haberman, S.M. Anderson, and M.J. Shlomchik. 2000. Germinal center initiation, variable gene region hypermutation, and mutant B cell selection without detectable immune complexes on follicular dendritic cells. *J Exp Med*. 192:931-942.
Hata, K., N. Yanase, K. Sudo, H. Kiyonari, Y. Mukumoto, J. Mizuguchi, and T. Yokosuka. 2016. Differential regulation of T-cell dependent and T-cell independent antibody responses through arginine methyltransferase PRMT1 in vivo. *FEBS Lett*. 590:1200-1210.
Heesters, B.A., R.C. Myers, and M.C. Carroll. 2014. Follicular dendritic cells: dynamic antigen libraries. *Nature Reviews Immunology*. 14:495-504.
Hombach, J., T. Tsubata, L. Leclercq, H. Stappert, and M. Reth. 1990. Molecular components of the B-cell antigen receptor complex of the IgM class. *Nature*. 343:760-762.
Hsu, W.J., M.C. Chiang, Y.C. Chao, Y.C. Chang, M.C. Hsu, C.H. Chung, I.L. Tsai, C.Y. Chu, H.C. Wu, C.C. Yang, C.C. Lee, and C.W. Lin. 2024. Arginine Methylation of DDX3 by PRMT1 Mediates Mitochondrial Homeostasis to Promote Breast Cancer Metastasis. *Cancer Res*. 84:3023-3043.

Inbar, D., J. Hochman, and D. Givol. 1972. Localization of antibody-combining sites within the variable portions of heavy and light chains. *Proc Natl Acad Sci U S A*. 69:2659-2662.
Infantino, S., B. Benz, T. Waldmann, M. Jung, R. Schneider, and M. Reth. 2010. Arginine methylation of the B cell antigen receptor promotes differentiation. *J Exp Med*. 207:711-719.
Infantino, S., A. Light, K. O'Donnell, V. Bryant, D.T. Avery, M. Elliott, S.G. Tangye, G. Belz, F. Mackay, S. Richard, and D. Tarlinton. 2017. Arginine methylation catalyzed by PRMT1 is required for B cell activation and differentiation. *Nat Commun*. 8:891.
Inoue, T., R. Shinnakasu, W. Ise, C. Kawai, T. Egawa, and T. Kurosaki. 2017. The transcription factor Foxo1 controls germinal center B cell proliferation in response to T cell help. *J Exp Med*. 214:1181-1198.
Jack, R.S., T. Imanishi-Kari, and K. Rajewsky. 1977. Idiotypic analysis of the response of C57BL/6 mice to the (4-hydroxy-3-nitrophenyl)acetyl group. *European Journal of Immunology*. 7:559-565.
Jacob, J., G. Kelsoe, K. Rajewsky, and U. Weiss. 1991. Intraclonal generation of antibody mutants in germinal centres. *Nature*. 354:389-392.
Jerne, N.K. 1951. A study of avidity based on rabbit skin responses to diphtheria toxin-antitoxin mixtures. *Acta Pathol Microbiol Scand Suppl (1926)*. 87:1-183.
Jin, H., R. Carrio, A. Yu, and T.R. Malek. 2004. Distinct Activation Signals Determine whether IL-21 Induces B Cell Costimulation, Growth Arrest, or Bim-Dependent Apoptosis1. *The Journal of Immunology*. 173:657-665.
Jung, D., and F.W. Alt. 2004. Unraveling V(D)J recombination; insights into gene regulation. *Cell*. 116:299-311.
Kallies, A., J. Hasbold, K. Fairfax, C. Pridans, D. Emslie, B.S. McKenzie, A.M. Lew, L.M. Corcoran, P.D. Hodgkin, D.M. Tarlinton, and S.L. Nutt. 2007. Initiation of plasma-cell differentiation is independent of the transcription factor Blimp-1. *Immunity*. 26:555-566.
Kato, Y., R.K. Abbott, B.L. Freeman, S. Haupt, B. Groschel, M. Silva, S. Menis, D.J. Irvine, W.R. Schief, and S. Crotty. 2020. Multifaceted Effects of Antigen Valency on B Cell Response Composition and Differentiation In Vivo. *Immunity*. 53:548-563.e548.
Khalil, M.I., H.M. Ismail, G. Panasyuk, A. Bdzhola, V. Filonenko, I. Gout, and O.E. Pardo. 2023. Asymmetric Dimethylation of Ribosomal S6 Kinase 2 Regulates Its Cellular Localisation and Pro-Survival Function. *Int J Mol Sci*. 24.
Khurana, S., E.M. Coyle, S. Verma, L.R. King, J. Manischewitz, C.J. Crevar, D.M. Carter, T.M. Ross, and H. Golding. 2014. H5 N-terminal β sheet promotes oligomerization of H7-HA1 that induces better antibody affinity maturation and enhanced protection against H7N7 and H7N9 viruses compared to inactivated influenza vaccine. *Vaccine*. 32:6421-6432.
Klein, U., S. Casola, G. Cattoretti, Q. Shen, M. Lia, T. Mo, T. Ludwig, K. Rajewsky, and R. Dalla-Favera. 2006. Transcription factor IRF4 controls plasma cell differentiation and class-switch recombination. *Nat Immunol*. 7:773-782.
Kwak, K., M. Akkaya, and S.K. Pierce. 2019. B cell signaling in context. *Nature Immunology*. 20:963-969.
Laidlaw, B.J., L. Duan, Y. Xu, S.E. Vazquez, and J.G. Cyster. 2020. The transcription factor Hhex cooperates with the corepressor Tle3 to promote memory B cell development. *Nat Immunol*. 21:1082-1093.
Le, T.V., T.H. Kim, and D.D. Chaplin. 2008. Intraclonal competition inhibits the formation of high-affinity antibody-secreting cells. *J Immunol*. 181:6027-6037.

Lee, J.H., H.J. Sutton, C.A. Cottrell, I. Phung, G. Ozorowski, L.M. Sewall, R. Nedellec, C. Nakao, M. Silva, S.T. Richey, J.L. Torres, W.-H. Lee, E. Georgeson, M. Kubitz, S. Hodges, T.-M. Mullen, Y. Adachi, K.M. Cirelli, A. Kaur, C. Allers, M. Fahlberg, B.F. Grasperge, J.P. Dufour, F. Schiro, P.P. Aye, O. Kalyuzhniy, A. Liguori, D.G. Carnathan, G. Silvestri, X. Shen, D.C. Montefiori, R.S. Veazey, A.B. Ward, L. Hangartner, D.R. Burton, D.J. Irvine, W.R. Schief, and S. Crotty. 2022. Long-primed germinal centres with enduring affinity maturation and clonal migration. *Nature*. 609:998-1004.

Leonard, S., N. Gordon, N. Smith, M. Rowe, P.G. Murray, and C.B. Woodman. 2012. Arginine Methyltransferases Are Regulated by Epstein-Barr Virus in B Cells and Are Differentially Expressed in Hodgkin's Lymphoma. *Pathogens*. 1:52-64.

Leung, W., M. Teater, C. Durmaz, C. Meydan, A.G. Chivu, A. Chadburn, E.J. Rice, A. Muley, J.M. Camarillo, J. Arivalagan, Z. Li, C.R. Flowers, N.L. Kelleher, C.G. Danko, M. Imielinski, S.S. Dave, S.A. Armstrong, C.E. Mason, and A.M. Melnick. 2022. SETD2 Haploinsufficiency Enhances Germinal Center-Associated AICDA Somatic Hypermutation to Drive B-cell Lymphomagenesis. *Cancer Discov*. 12:1782-1803.

Linterman, M.A., L. Beaton, D. Yu, R.R. Ramiscal, M. Srivastava, J.J. Hogan, N.K. Verma, M.J. Smyth, R.J. Rigby, and C.G. Vinuesa. 2010. IL-21 acts directly on B cells to regulate Bcl-6 expression and germinal center responses. *J Exp Med*. 207:353-363.

Linterman, M.A., W. Pierson, S.K. Lee, A. Kallies, S. Kawamoto, T.F. Rayner, M. Srivastava, D.P. Divekar, L. Beaton, J.J. Hogan, S. Fagarasan, A. Liston, K.G. Smith, and C.G. Vinuesa. 2011. Foxp3+ follicular regulatory T cells control the germinal center response. *Nat Med*. 17:975-982.

Litzler, L.C., A. Zahn, K.L. Dionne, A. Sprumont, S.R. Ferreira, M.R.F. Slattery, S.P. Methot, A.-M. Patenaude, S. Hébert, N. Kabir, P.G. Subramani, S. Jung, S. Richard, C.L. Kleinman, and J.M. Di Noia. 2023. Protein arginine methyltransferase 1 regulates B cell fate after positive selection in the germinal center in mice. *Journal of Experimental Medicine*. 220:e20220381.

Litzler, L.C., A. Zahn, A.P. Meli, S. Hébert, A.-M. Patenaude, S.P. Methot, A. Sprumont, T. Bois, D. Kitamura, S. Costantino, I.L. King, C.L. Kleinman, S. Richard, and J.M. Di Noia. 2019. PRMT5 is essential for B cell development and germinal center dynamics. *Nature Communications*. 10:22.

Liu, J., X. Bu, C. Chu, X. Dai, J.M. Asara, P. Sicinski, G.J. Freeman, and W. Wei. 2023. PRMT1 mediated methylation of cGAS suppresses anti-tumor immunity. *Nature Communications*. 14:2806.

Long, Z., B. Phillips, D. Radtke, M. Meyer-Hermann, and O. Bannard. 2022. Competition for refueling rather than cyclic reentry initiation evident in germinal centers. *Sci Immunol*. 7:eabm0775.

Lu, L.L., T.J. Suscovich, S.M. Fortune, and G. Alter. 2018. Beyond binding: antibody effector functions in infectious diseases. *Nature Reviews Immunology*. 18:46-61.

Luo, W., L. Conter, R.A. Elsner, S. Smita, F. Weisel, D. Callahan, S. Wu, M. Chikina, and M. Shlomchik. 2023. IL-21R signal reprogramming cooperates with CD40 and BCR signals to select and differentiate germinal center B cells. *Sci Immunol*. 8:eadd1823.

Ma, X.M., and J. Blenis. 2009. Molecular mechanisms of mTOR-mediated translational control. *Nature Reviews Molecular Cell Biology*. 10:307-318.

Martin, J.T., C.A. Cottrell, A. Antanasijevic, D.G. Carnathan, B.J. Cossette, C.A. Enemuo, E.H. Gebru, Y. Choe, F. Viviano, S. Fischinger, T. Tokatlian, K.M. Cirelli, G. Ueda, J. Copps,

T. Schiffner, S. Menis, G. Alter, W.R. Schief, S. Crotty, N.P. King, D. Baker, G. Silvestri, A.B. Ward, and D.J. Irvine. 2020. Targeting HIV Env immunogens to B cell follicles in nonhuman primates through immune complex or protein nanoparticle formulations. *NPJ Vaccines*. 5:72.

Martin, P.L., F.J. Pérez-Areales, S.V. Rao, S.J. Walsh, J.S. Carroll, and D.R. Spring. 2024. Towards the Targeted Protein Degradation of PRMT1. *ChemMedChem*. 19:e202400269.

Martínez-Riaño, A., S. Wang, S. Boeing, S. Minoughan, A. Casal, K.M. Spillane, B. Ludewig, and P. Tolar. 2023. Long-term retention of antigens in germinal centers is controlled by the spatial organization of the follicular dendritic cell network. *Nat Immunol*. 24:1281-1294.

McBride, K.M., A. Gazumyan, E.M. Woo, V.M. Barreto, D.F. Robbiani, B.T. Chait, and M.C. Nussenzweig. 2006. Regulation of hypermutation by activation-induced cytidine deaminase phosphorylation. *Proceedings of the National Academy of Sciences*. 103:8798-8803.

McBride, K.M., A. Gazumyan, E.M. Woo, T.A. Schwickert, B.T. Chait, and M.C. Nussenzweig. 2008. Regulation of class switch recombination and somatic mutation by AID phosphorylation. *Journal of Experimental Medicine*. 205:2585-2594.

Mehta, D.S., A.L. Wurster, M.J. Whitters, D.A. Young, M. Collins, and M.J. Grusby. 2003. IL-21 induces the apoptosis of resting and activated primary B cells. *J Immunol*. 170:4111-4118.

Merkenschlager, J., R.-M. Berz, V. Ramos, M. Uhlig, A.J. MacLean, C.R. Nowosad, T.Y. Oliveira, and M.C. Nussenzweig. 2023. Continually recruited naïve T cells contribute to the follicular helper and regulatory T cell pools in germinal centers. *Nature Communications*. 14:6944.

Mestas, J., and C.C.W. Hughes. 2004. Of Mice and Not Men: Differences between Mouse and Human Immunology. *The Journal of Immunology*. 172:2731-2738.

Meyer, S.J., M. Steffensen, A. Acs, T. Weisenburger, C. Wadewitz, T.H. Winkler, and L. Nitschke. 2021. CD22 Controls Germinal Center B Cell Receptor Signaling, Which Influences Plasma Cell and Memory B Cell Output. *J Immunol*. 207:1018-1032.

Mlynarczyk, C., M. Teater, J. Pae, C.R. Chin, L. Wang, T. Arulraj, D. Barisic, A. Papin, K.B. Hoehn, E. Kots, J. Ersching, A. Bandyopadhyay, E. Barin, H.X. Poh, C.M. Evans, A. Chadburn, Z. Chen, H. Shen, H.M. Isles, B. Pelzer, I. Tsialta, A.S. Doane, H. Geng, M.H. Rehman, J. Melnick, W. Morgan, D.T.T. Nguyen, O. Elemento, M.G. Kharas, S.R. Jaffrey, D.W. Scott, G. Khelashvili, M. Meyer-Hermann, G.D. Victora, and A. Melnick. 2023. BTG1 mutation yields supercompetitive B cells primed for malignant transformation. *Science*. 379:eabj7412.

Mond, J.J., A. Lees, and C.M. Snapper. 1995. T cell-independent antigens type 2. *Annu Rev Immunol*. 13:655-692.

Muramatsu, M., K. Kinoshita, S. Fagarasan, S. Yamada, Y. Shinkai, and T. Honjo. 2000. Class switch recombination and hypermutation require activation-induced cytidine deaminase (AID), a potential RNA editing enzyme. *Cell*. 102:553-563.

Nguyen, H.P., E. Liu, B.A. Walker, and N.T. Tran. 2023. Synergistic Effects of Type I PRMT1 and Type II PRMT5 Inhibitors Against Multiple Myeloma. *Blood*. 142:6593-6593.

Nieuwenhuis, P., and D. Opstelten. 1984. Functional anatomy of germinal centers. *Am J Anat*. 170:421-435.

Nojima, T., K. Haniuda, T. Moutai, M. Matsudaira, S. Mizokawa, I. Shiratori, T. Azuma, and D. Kitamura. 2011. In-vitro derived germinal centre B cells differentially generate memory B or plasma cells in vivo. *Nature Communications*. 2:465.

Nossal, G.J., G.L. Ada, and C.M. Austin. 1964. ANTIGENS IN IMMUNITY. IV. CELLULAR LOCALIZATION OF 125-I- AND 131-I-LABELLED FLAGELLA IN LYMPH NODES. *Aust J Exp Biol Med Sci*. 42:311-330.

Nothelfer, K., P.J. Sansonetti, and A. Phalipon. 2015. Pathogen manipulation of B cells: the best defence is a good offence. *Nature Reviews Microbiology*. 13:173-184.

Nowosad, C.R., L. Mesin, T.B.R. Castro, C. Wichmann, G.P. Donaldson, T. Araki, A. Schiepers, A.A.K. Lockhart, A.M. Bilate, D. Mucida, and G.D. Victora. 2020. Tunable dynamics of B cell selection in gut germinal centres. *Nature*. 588:321-326.

Okada, T., M.J. Miller, I. Parker, M.F. Krummel, M. Neighbors, S.B. Hartley, A. O'Garra, M.D. Cahalan, and J.G. Cyster. 2005. Antigen-engaged B cells undergo chemotaxis toward the T zone and form motile conjugates with helper T cells. *PLoS Biol*. 3:e150.

Oksenhendler, E., L. Gérard, C. Fieschi, M. Malphettes, G. Mouillot, R. Jaussaud, J.F. Viallard, M. Gardembas, L. Galicier, N. Schleinitz, F. Suarez, P. Soulas-Sprauel, E. Hachulla, A. Jaccard, A. Gardeur, I. Théodorou, C. Rabian, and P. Debré. 2008. Infections in 252 patients with common variable immunodeficiency. *Clin Infect Dis*. 46:1547-1554.

Oostindie, S.C., G.A. Lazar, J. Schuurman, and P.W.H.I. Parren. 2022. Avidity in antibody effector functions and biotherapeutic drug design. *Nature Reviews Drug Discovery*. 21:715-735.

Pae, J., J. Ersching, T.B.R. Castro, M. Schips, L. Mesin, S.J. Allon, J. Ordovas-Montanes, C. Mlynarczyk, A. Melnick, A. Efeyan, A.K. Shalek, M. Meyer-Hermann, and G.D. Victora. 2021. Cyclin D3 drives inertial cell cycling in dark zone germinal center B cells. *J Exp Med*. 218.

Panwar, V., A. Singh, M. Bhatt, R.K. Tonk, S. Azizov, A.S. Raza, S. Sengupta, D. Kumar, and M. Garg. 2023. Multifaceted role of mTOR (mammalian target of rapamycin) signaling pathway in human health and disease. *Signal Transduction and Targeted Therapy*. 8:375.

Peled, J.U., F.L. Kuang, M.D. Iglesias-Ussel, S. Roa, S.L. Kalis, M.F. Goodman, and M.D. Scharff. 2008. The biochemistry of somatic hypermutation. *Annu Rev Immunol*. 26:481-511.

Perlmutter, R.M., D. Hansburg, D.E. Briles, R.A. Nicolotti, and J.M. David. 1978. Subclass Restriction of Murine Anti-Carbohydrate Antibodies1. *The Journal of Immunology*. 121:566-572.

Petersone, L., C.J. Wang, N.M. Edner, A. Fabri, S.A. Nikou, C. Hinze, E.M. Ross, E. Ntavli, Y. Elfaki, F. Heuts, V. Ovcinnikovs, A. Rueda Gonzalez, L.P. Houghton, H.M. Li, Y. Zhang, K.M. Toellner, and L.S.K. Walker. 2023. IL-21 shapes germinal center polarization via light zone B cell selection and cyclin D3 upregulation. *J Exp Med*. 220.

Phan, T.G., D. Paus, T.D. Chan, M.L. Turner, S.L. Nutt, A. Basten, and R. Brink. 2006. High affinity germinal center B cells are actively selected into the plasma cell compartment. *J Exp Med*. 203:2419-2424.

Porter, R.R. 1959. The hydrolysis of rabbit y-globulin and antibodies with crystalline papain. *Biochem J*. 73:119-126.

Quinti, I., A. Soresina, G. Spadaro, S. Martino, S. Donnanno, C. Agostini, P. Claudio, D. Franco, A. Maria Pesce, F. Borghese, A. Guerra, R. Rondelli, and A. Plebani. 2007. Long-term

follow-up and outcome of a large cohort of patients with common variable immunodeficiency. *J Clin Immunol*. 27:308-316.
Randall, T.D., and R.E. Mebius. 2014. The development and function of mucosal lymphoid tissues: a balancing act with micro-organisms. *Mucosal Immunology*. 7:455-466.
Read, K.A., S.A. Amici, S. Farsi, M. Cutcliffe, B. Lee, C.-W.J. Lio, H.-J.J. Wu, M. Guerau-de-Arellano, and K.J. Oestreich. 2024. PRMT5 Promotes T follicular helper Cell Differentiation and Germinal Center Responses during Influenza Virus Infection. *The Journal of Immunology*. 212:1442-1449.
Rees, A.R. 2020. Understanding the human antibody repertoire. *MAbs*. 12:1729683.
Reif, K., E.H. Ekland, L. Ohl, H. Nakano, M. Lipp, R. Förster, and J.G. Cyster. 2002. Balanced responsiveness to chemoattractants from adjacent zones determines B-cell position. *Nature*. 416:94-99.
Revy, P., T. Muto, Y. Levy, F. Geissmann, A. Plebani, O. Sanal, N. Catalan, M. Forveille, R. Dufourcq-Labelouse, A. Gennery, I. Tezcan, F. Ersoy, H. Kayserili, A.G. Ugazio, N. Brousse, M. Muramatsu, L.D. Notarangelo, K. Kinoshita, T. Honjo, A. Fischer, and A. Durandy. 2000. Activation-induced cytidine deaminase (AID) deficiency causes the autosomal recessive form of the Hyper-IgM syndrome (HIGM2). *Cell*. 102:565-575.
Rivas, M.A., C. Meydan, C.R. Chin, M.F. Challman, D. Kim, B. Bhinder, A. Kloetgen, A.D. Viny, M.R. Teater, D.R. McNally, A.S. Doane, W. Béguelin, M.T.C. Fernández, H. Shen, X. Wang, R.L. Levine, Z. Chen, A. Tsirigos, O. Elemento, C.E. Mason, and A.M. Melnick. 2021. Smc3 dosage regulates B cell transit through germinal centers and restricts their malignant transformation. *Nat Immunol*. 22:240-253.
Ruddle, N.H., and E.M. Akirav. 2009. Secondary Lymphoid Organs: Responding to Genetic and Environmental Cues in Ontogeny and the Immune Response1. *The Journal of Immunology*. 183:2205-2212.
Schmitz, R., G.W. Wright, D.W. Huang, C.A. Johnson, J.D. Phelan, J.Q. Wang, S. Roulland, M. Kasbekar, R.M. Young, A.L. Shaffer, D.J. Hodson, W. Xiao, X. Yu, Y. Yang, H. Zhao, W. Xu, X. Liu, B. Zhou, W. Du, W.C. Chan, E.S. Jaffe, R.D. Gascoyne, J.M. Connors, E. Campo, A. Lopez-Guillermo, A. Rosenwald, G. Ott, J. Delabie, L.M. Rimsza, K.T.K. Wei, A.D. Zelenetz, J.P. Leonard, N.L. Bartlett, B. Tran, J. Shetty, Y. Zhao, D.R. Soppet, S. Pittaluga, W.H. Wilson, and L.M. Staudt. 2018. Genetics and Pathogenesis of Diffuse Large B-Cell Lymphoma. *New England Journal of Medicine*. 378:1396-1407.
Sciammas, R., A.L. Shaffer, J.H. Schatz, H. Zhao, L.M. Staudt, and H. Singh. 2006. Graded expression of interferon regulatory factor-4 coordinates isotype switching with plasma cell differentiation. *Immunity*. 25:225-236.
Sen, S., Z. He, S. Ghosh, K.J. Dery, L. Yang, J. Zhang, and Z. Sun. 2018. PRMT1 Plays a Critical Role in Th17 Differentiation by Regulating Reciprocal Recruitment of STAT3 and STAT5. *J Immunol*. 201:440-450.
Shaffer, A.L., M. Shapiro-Shelef, N.N. Iwakoshi, A.H. Lee, S.B. Qian, H. Zhao, X. Yu, L. Yang, B.K. Tan, A. Rosenwald, E.M. Hurt, E. Petroulakis, N. Sonenberg, J.W. Yewdell, K. Calame, L.H. Glimcher, and L.M. Staudt. 2004. XBP1, downstream of Blimp-1, expands the secretory apparatus and other organelles, and increases protein synthesis in plasma cell differentiation. *Immunity*. 21:81-93.
Shinnakasu, R., T. Inoue, K. Kometani, S. Moriyama, Y. Adachi, M. Nakayama, Y. Takahashi, H. Fukuyama, T. Okada, and T. Kurosaki. 2016. Regulated selection of germinal-center cells into the memory B cell compartment. *Nature Immunology*. 17:861-869.

Sloan, S.L., F. Brown, M. Long, C. Weigel, S. Koirala, J.-H. Chung, B. Pray, L. Villagomez, C. Hinterschied, A. Sircar, J. Helmig-Mason, A. Prouty, E. Brooks, Y. Youssef, W. Hanel, S. Parekh, W.K. Chan, Z. Chen, R. Lapalombella, L. Sehgal, K. Vaddi, P. Scherle, S. Chen-Kiang, M. Di Liberto, O. Elemento, C. Meydan, J. Foox, D. Butler, C.E. Mason, R.A. Baiocchi, and L. Alinari. 2023. PRMT5 supports multiple oncogenic pathways in mantle cell lymphoma. *Blood*. 142:887-902.

Smith, K.G., A. Light, G.J. Nossal, and D.M. Tarlinton. 1997. The extent of affinity maturation differs between the memory and antibody-forming cell compartments in the primary immune response. *Embo j*. 16:2996-3006.

Sprumont, A., A. Rodrigues, S.J. McGowan, C. Bannard, and O. Bannard. 2023. Germinal centers output clonally diverse plasma cell populations expressing high- and low-affinity antibodies. *Cell*. 186:5486-5499.e5413.

Sundling, C., A.W.Y. Lau, K. Bourne, C. Young, C. Laurianto, J.R. Hermes, R.J. Menzies, D. Butt, N.J. Kräutler, D. Zahra, D. Suan, and R. Brink. 2021. Positive selection of IgG(+) over IgM(+) B cells in the germinal center reaction. *Immunity*. 54:988-1001.e1005.

Sutton, H.J., X. Gao, H.G. Kelly, B.J. Parker, M. Lofgren, C. Dacon, D. Chatterjee, R.A. Seder, J. Tan, A.H. Idris, T. Neeman, and I.A. Cockburn. 2024. Lack of affinity signature for germinal center cells that have initiated plasma cell differentiation. *Immunity*. 57:245-255.e245.

Suzuki, K., I. Grigorova, T.G. Phan, L.M. Kelly, and J.G. Cyster. 2009. Visualizing B cell capture of cognate antigen from follicular dendritic cells. *Journal of Experimental Medicine*. 206:1485-1493.

Szakal, A.K., M.H. Kosco, and J.G. Tew. 1989. Microanatomy of lymphoid tissue during humoral immune responses: structure function relationships. *Annu Rev Immunol*. 7:91-109.

Tang, J., A. Frankel, R.J. Cook, S. Kim, W.K. Paik, K.R. Williams, S. Clarke, and H.R. Herschman. 2000. PRMT1 is the predominant type I protein arginine methyltransferase in mammalian cells. *J Biol Chem*. 275:7723-7730.

Tang, J., S. Ravichandran, Y. Lee, G. Grubbs, E.M. Coyle, L. Klenow, H. Genser, H. Golding, and S. Khurana. 2021. Antibody affinity maturation and plasma IgA associate with clinical outcome in hospitalized COVID-19 patients. *Nature Communications*. 12:1221.

Tikhanovich, I., J. Zhao, B. Bridges, S. Kumer, B. Roberts, and S.A. Weinman. 2017. Arginine methylation regulates c-Myc–dependent transcription by altering promoter recruitment of the acetyltransferase p300. *Journal of Biological Chemistry*. 292:13333-13344.

Turner, C.A., Jr., D.H. Mack, and M.M. Davis. 1994. Blimp-1, a novel zinc finger-containing protein that can drive the maturation of B lymphocytes into immunoglobulin-secreting cells. *Cell*. 77:297-306.

Turqueti-Neves, A., M. Otte, O. Prazeres da Costa, U.E. Höpken, M. Lipp, T. Buch, and D. Voehringer. 2014. B-cell-intrinsic STAT6 signaling controls germinal center formation. *Eur J Immunol*. 44:2130-2138.

Tyagi, R., S. Basu, A. Dhar, S. Gupta, S.L. Gupta, and R.K. Jaiswal. 2023. Role of Immunoglobulin A in COVID-19 and Influenza Infections. *Vaccines (Basel)*. 11.

van Galen, J.C., R.P. Kuiper, L. van Emst, M. Levers, E. Tijchon, B. Scheijen, E. Waanders, S.V. van Reijmersdal, C. Gilissen, A.G. van Kessel, P.M. Hoogerbrugge, and F.N. van

Leeuwen. 2010. BTG1 regulates glucocorticoid receptor autoinduction in acute lymphoblastic leukemia. *Blood*. 115:4810-4819.
Verma, S., M. Dimitrova, A. Munjal, J. Fontana, J. Crevar Corey, M. Carter Donald, M. Ross Ted, S. Khurana, and H. Golding. 2012. Oligomeric Recombinant H5 HA1 Vaccine Produced in Bacteria Protects Ferrets from Homologous and Heterologous Wild-Type H5N1 Influenza Challenge and Controls Viral Loads Better than Subunit H5N1 Vaccine by Eliciting High-Affinity Antibodies. *Journal of Virology*. 86:12283-12293.
Viant, C., G.H.J. Weymar, A. Escolano, S. Chen, H. Hartweger, M. Cipolla, A. Gazumyan, and M.C. Nussenzweig. 2020. Antibody Affinity Shapes the Choice between Memory and Germinal Center B Cell Fates. *Cell*. 183:1298-1311.e1211.
Victora, G.D., D. Dominguez-Sola, A.B. Holmes, S. Deroubaix, R. Dalla-Favera, and M.C. Nussenzweig. 2012. Identification of human germinal center light and dark zone cells and their relationship to human B-cell lymphomas. *Blood*. 120:2240-2248.
Victora, G.D., and M.C. Nussenzweig. 2012. Germinal Centers. *Annual Review of Immunology*. 30:429-457.
Victora, G.D., T.A. Schwickert, D.R. Fooksman, A.O. Kamphorst, M. Meyer-Hermann, M.L. Dustin, and M.C. Nussenzweig. 2010. Germinal center dynamics revealed by multiphoton microscopy with a photoactivatable fluorescent reporter. *Cell*. 143:592-605.
Weigert, M.G., I.M. Cesari, S.J. Yonkovich, and M. Cohn. 1970. Variability in the Lambda Light Chain Sequences of Mouse Antibody. *Nature*. 228:1045-1047.
Weinstein, J.S., E.I. Herman, B. Lainez, P. Licona-Limón, E. Esplugues, R. Flavell, and J. Craft. 2016. TFH cells progressively differentiate to regulate the germinal center response. *Nat Immunol*. 17:1197-1205.
Wu, H., Y. Deng, Y. Feng, D. Long, K. Ma, X. Wang, M. Zhao, L. Lu, and Q. Lu. 2018. Epigenetic regulation in B-cell maturation and its dysregulation in autoimmunity. *Cellular & Molecular Immunology*. 15:676-684.
Wurster, A.L., V.L. Rodgers, M.F. White, T.L. Rothstein, and M.J. Grusby. 2002. Interleukin-4-mediated protection of primary B cells from apoptosis through Stat6-dependent up-regulation of Bcl-xL. *J Biol Chem*. 277:27169-27175.
Xu-Monette, Z.Y., Q. Deng, G.C. Manyam, A. Tzankov, L. Li, Y. Xia, X.-x. Wang, D. Zou, C. Visco, K. Dybkær, J. Li, L. Zhang, H. Liang, S. Montes-Moreno, A. Chiu, A. Orazi, Y. Zu, G. Bhagat, K.L. Richards, E.D. Hsi, W.W.L. Choi, J.H. van Krieken, J. Huh, M. Ponzoni, A.J.M. Ferreri, B.M. Parsons, M.B. Møller, S.A. Wang, R.N. Miranda, M.A. Piris, J.N. Winter, L.J. Medeiros, Y. Li, and K.H. Young. 2016. Clinical and Biologic Significance of MYC Genetic Mutations in De Novo Diffuse Large B-cell Lymphoma. *Clinical Cancer Research*. 22:3593-3605.
Yamagata, K., H. Daitoku, Y. Takahashi, K. Namiki, K. Hisatake, K. Kako, H. Mukai, Y. Kasuya, and A. Fukamizu. 2008. Arginine Methylation of FOXO Transcription Factors Inhibits Their Phosphorylation by Akt. *Molecular Cell*. 32:221-231.
Yang, L., L. Miao, F. Liang, H. Huang, X. Teng, S. Li, J. Nuriddinov, M.E. Selzer, and Y. Hu. 2014. The mTORC1 effectors S6K1 and 4E-BP play different roles in CNS axon regeneration. *Nature Communications*. 5:5416.
Yang, M., Y. Zhang, G. Liu, Z. Zhao, J. Li, L. Yang, K. Liu, W. Hu, Y. Lou, J. Jiang, Q. Liu, and P. Zhao. 2022. TIPE1 inhibits osteosarcoma tumorigenesis and progression by regulating PRMT1 mediated STAT3 arginine methylation. *Cell Death & Disease*. 13:815.

Yeh, C.-H., T. Nojima, M. Kuraoka, and G. Kelsoe. 2018. Germinal center entry not selection of B cells is controlled by peptide-MHCII complex density. *Nature Communications*. 9:928.

Ying, Z., M. Mei, P. Zhang, C. Liu, H. He, F. Gao, and S. Bao. 2015. Histone Arginine Methylation by PRMT7 Controls Germinal Center Formation via Regulating Bcl6 Transcription. *The Journal of Immunology*. 195:1538-1547.

Young, C., and R. Brink. 2021. The unique biology of germinal center B cells. *Immunity*. 54:1652-1664.

Yu, Z., T. Chen, J. Hébert, E. Li, and S. Richard. 2009. A mouse PRMT1 null allele defines an essential role for arginine methylation in genome maintenance and cell proliferation. *Mol Cell Biol*. 29:2982-2996.

Yuniati, L., L.T. van der Meer, E. Tijchon, D. van Ingen Schenau, L. van Emst, M. Levers, S.A. Palit, C. Rodenbach, G. Poelmans, P.M. Hoogerbrugge, J. Shan, M.S. Kilberg, B. Scheijen, and F.N. van Leeuwen. 2016. Tumor suppressor BTG1 promotes PRMT1-mediated ATF4 function in response to cellular stress. *Oncotarget*. 7:3128-3143.

Zahn, A., M. Daugan, S. Safavi, D. Godin, C. Cheong, A. Lamarre, and J.M. Di Noia. 2013. Separation of Function between Isotype Switching and Affinity Maturation In Vivo during Acute Immune Responses and Circulating Autoantibodies in UNG-Deficient Mice. *The Journal of Immunology*. 190:5949-5960.

Zhang, S., J. Gu, L.-l. Shi, B. Qian, X. Diao, X. Jiang, J. Wu, Z. Wu, and A. Shen. 2023. A pan-cancer analysis of anti-proliferative protein family genes for therapeutic targets in cancer. *Scientific Reports*. 13:21607.

Zheng, S., J. Moehlenbrink, Y.C. Lu, L.P. Zalmas, C.A. Sagum, S. Carr, J.F. McGouran, L. Alexander, O. Fedorov, S. Munro, B. Kessler, M.T. Bedford, Q. Yu, and N.B. La Thangue. 2013. Arginine methylation-dependent reader-writer interplay governs growth control by E2F-1. *Mol Cell*. 52:37-51.

Zhu, F., H. Guo, P.D. Bates, S. Zhang, H. Zhang, K.J. Nomie, Y. Li, L. Lu, K.R. Seibold, F. Wang, I. Rumball, H. Cameron, N.M. Hoang, D.T. Yang, W. Xu, L. Zhang, M. Wang, C.M. Capitini, and L. Rui. 2019. PRMT5 is upregulated by B-cell receptor signaling and forms a positive-feedback loop with PI3K/AKT in lymphoma cells. *Leukemia*. 33:2898-2911.

Zhu, J., L. Guo, C.J. Watson, J. Hu-Li, and W.E. Paul. 2001. Stat6 Is Necessary and Sufficient for IL-4's Role in Th2 Differentiation and Cell Expansion. *The Journal of Immunology*. 166:7276-7281.

Zotos, D., J.M. Coquet, Y. Zhang, A. Light, K. D'Costa, A. Kallies, L.M. Corcoran, D.I. Godfrey, K.-M. Toellner, M.J. Smyth, S.L. Nutt, and D.M. Tarlinton. 2010. IL-21 regulates germinal center B cell differentiation and proliferation through a B cell–intrinsic mechanism. *Journal of Experimental Medicine*. 207:365-378.

Zotos, D., I. Quast, C.S.N. Li-Wai-Suen, C.I. McKenzie, M.J. Robinson, A. Kan, G.K. Smyth, P.D. Hodgkin, and D.M. Tarlinton. 2021. The concerted change in the distribution of cell cycle phases and zone composition in germinal centers is regulated by IL-21. *Nature Communications*. 12:7160.